FINAL REPORT

SIMULATION STUDIES OF THE APPLICATION OF SEASAT DATA IN WEATHER AND STATE OF SEA FORECASTING MODELS

Vincent J. Cardone

J. Arthur Greenwood

Oceanweather Inc.
170 Hamilton Avenue
White Plains, New York 10601

Submitted to

Laboratory for Atmospheric Sciences
Modelling and Simulation Facility
National Aeronautics and Space Administration
Goddard Space Flight Center
Greenbelt, Maryland 20771

Contract NAS5-24498

October, 1979

Table of Contents

1. INTRODUCTION

SEASAT-A was launched on 26 June, 1978 carrying a complement of active and passive microwave instruments designed to sense the vector wind stress at the sea surface, the significant wave height and other atmospheric and oceanographic surface properties. The satellite stopped transmitting after acquiring global data from each instrument over a 99 day period. A preliminary overview of the SEASAT-A mission has been reported by Born et al. (1979a).

The evaluation of the spacecraft and sensor performance must still be regarded to be in a preliminary stage. Nevertheless, on the basis of intensive analysis of limited geophysical series, derived from sensor records by a set of geophysical retrieval algorithms developed before launch, it is apparent that the design goals for measurement accuracy will be met, at least for those sensors of interest here (Born et al., 1979b). The research program, of which this study is a part, is concerned primarily with radar backscatter measurements from the scatterometer (SASS) and wind vectors (affected by aliases) derived therefrom; with scalar winds derived from the passive microwave measurements by the multichannel radiometer (SMMR); and with significant wave height measurements from the radar altimeter (ALT).

Quantitative wind and surface wave data, available on a global basis, shall have great potential for improving our knowledge of and ability to predict weather and sea state through the improved specification of initial conditions for numerical weather and ocean models. However, because of the novel nature of such synoptic data it is not known exactly how the data should be used to achieve maximum impact, how much improvement in environmental forecasts can be expected, or how best to exploit SEASAT measurement capabilities in a future operational system.

Following the refinement and evaluation of algorithms for retrieval of geophysical data from seasat sensor data, global wind and wave data sets will be made available to the scientific community for studies directed toward resolution of the above

questions. Prior to the availability of real data sets, however, answers to the above questions can be sought through simulation experiments carried out with general circulation (GCM) models and coupled ocean-GCM models. Such experiments should also lead to the development of optimum techniques for the assimilation of real SEASAT-A data into numerical weather and sea state forecasting models.

The very first SEASAT simulation experiments began in 1975 and were conducted at the Goddard Institute of Space Studies (GISS) as a collaborative effort involving several groups, as reported by Cardone (1977) and Halem et al. (1976). This study describes more recent results of the collaborative program with particular emphasis on three areas in which Oceanweather Inc. contributed significantly: (1) the design and analysis of SEASAT simulation studies in which the error structure of conventional analyses and forecasts is modeled realistically; (2) the development and implementation on the GMSF computer of a global spectral ocean wave model (GSOWM) which may be run in tandem with the GMSF GCM to assimilate SEASAT data and assess forecast sea state impacts; (3) the design of algorithms for the assimilation of SASS wind data into the GMSF GCM and for the utilization of real SASS wind data and ALT wave height data in a coupled GCM-GSOWM.

2. SEASAT SIMULATION STUDIES

2.1 Background

A general experimental design for SEASAT simulation studies has been formulated through the efforts of a group of scientists engaged in general circulation modelling, numerical weather prediction, and SEASAT-related research. The group first met at the National Center for Atmospheric Research (NCAR) in February of 1975, and produced an overall plan of action that suggested near-term, intermediate, and long-range goals. The group now serves as an ad hoc SEASAT simulation studies steering group and meets periodically to review results of the simulation studies and to participate in the refinement and evaluation of the experiment plan.

The first experiments suggested were of the so-called identical-twin type, in which a specific general circulation model provides both the "real" atmosphere reference data and the simulated satellite data, and is used to assimilate the satellite data to study the impact of such assimilation on subsequent forecasts. Those experiments were to simulate SEASAT-A, and a possible multiple SEASAT operational system, and were to involve straightforward insertion of simulated SEASAT wind measurements both alone and with simulated temperature-sounding data.

Experiments designed largely along those lines were performed at GISS with the GISS GCM during 1976. The results of those experiments have been reported in detail by Halem et al. (1976) and Cardone (1977) and McCandless and Cardone (1976). The results of those first experiments were mildly encouraging but were regarded with great caution because of the well known shortcomings of the experimental methods employed. In particular, the experiment was biased toward optimistic results because the identical GCM had been used in all three runs that comprised the simulation study. Also, the random nature of the error specification used to model operational (not enhanced by SEASAT) analyses did not realistically simulate the error structure in real analyses based upon the conventional observation network. Finally, the

asynoptic nature of SEASAT data was not modelled and the method used to assimilate the data was very crude.

Following those experiments, a detailed plan for SEASAT simulation experiments was drafted in collaboration with key members of the steering group. The plan called for a major redesign of the simulation impact tests from the methodology that had been employed in most prior satellite simulation studies. In particular it recommended the simulation in great detail, of the conventional meteorological observing network and the conventional methods for objectively analysing the observations from such network to produce initial states for numerical weather forecasting, with the goal of realistically simulating the error characteristics of conventional meteorological data fields and, thence, the forecast error growth rates found in nature. The realistic control states so produced were to be used to assimilate simulated SEASAT data asymptotically.

The plan called for relatively simple SEASAT simulation experiments at first, e.g. the direct insertion of perfect SEASAT-derived winds, following a SEASAT-A orbit, at the lowest active level of the GISS GCM, i.e. Level 9. Experiments to follow were to include simulation of the improvements in marine surface pressure to be expected to accompany the SEASAT winds; insertion of all satellite data (e.g. VTPR, GOES winds); and simulation of possible future configurations of satellite orbits and sensors. Also, it was proposed that a sea-state forecast model be coupled to the GCM, to allow assessment of the impact on wave forecasts to follow from indicated levels of impact on weather forecasts. The evolution of simulation experiments was to proceed to the use of more sophisticated assimilation methods, and ultimately to experiments with real SEASAT-A data.

2.2 Summary of Results

Significant progress has been made to date toward the achievement of the objectives stated above. A set of simulation studies has been completed, using the GMSF GCM, which modelled the error structure in conventional analyses and forecasts far

more realistically than has been done in prior studies. It has been possible to demonstrate, rather convincingly, that against such control analyses and forecasts, SEASAT surface wind data have the potential to improve numerical weather forecasts significantly over extratropical ocean and land areas.

The detailed results of the realistic simulations have been documented and submitted for publication in revised form as a paper entitled:

> "Observing Systems Simulation and Potential Impact of Marine Surface Wind Data on Numerical Weather Prediction" by M. Cane, V. Cardone, M. Halem, I. Halberstam, J. Ulrich (Submitted to Mon. Wea. Rev.)

A copy of the paper is attached to this report as Appendix C. Only a summary of results is given here.

A simulation experiment requires four elements: [1] a "nature run", i.e. a month-long integration of the GCM from an arbitrary initial state, to provide a complete record of the state of the model atmosphere, which is used both to fabricate "observational" reports and to evaluate analyses and forecasts; [2] a control assimilation that is like an operational forecast-analysis cycle based on conventional observations, except that the data used to produce the analyses and fields are in fact fabricated from the nature run; [3] a SEASAT assimilation, differing from the control assimilation in incorporating "SEASAT data" (likewise fabricated from the nature run) in the forecast-analysis cycle' [4] forecasts produced from both initial conditions [2] & [3], which are compared to nature and inter se to provide an assessment of the anticipated impact of the SEASAT data.

In the most recent series of simulations, a 30-day history run with the GMSF GCM was used to fabricate simulated observations at the times and locations of the individual conventional reports (surface, radiosonde, and ship) actually received during February 1976. Those fabricated observations, suitably degraded for instrument and sampling errors, were then used to create analysed fields on the GCM grid in an analysis-forecast cycle like those in use

at major meteorological centers. The control fields so produced are much more representative of actual analyses than those produced by perturbing initial states with random errors. The forecast error growth in five simulated 72-hour forecasts from the control states was gratifyingly similar to that found in operational numerical forecasts.

A series of experiments has been conducted, each simulating the addition of surface winds derived from SEASAT-A to the control run. In all those experiments, the SEASAT winds were fabricated directly for the GCM grid points intercepted by the SEASAT-A scatterometer swath, and representative of the lowest level of the GCM (about 950 mb). Two of the experiments assumed error-free SEASAT winds: the first assimilated wind data asynoptically by the direct insertion method (PW-DIM); the second employed the successive correction method (PW-SCM). An experiment was also performed which simulated the addition of perfect sounder derived temperatures by the SCM (PT-SCM) to the control, so that the relative impact of surface wind data compared to sounder data (both error free) could be assessed. The results of forecast experiments from each of these experiments are compared briefly here. (A more detailed discussion is contained in Appendix C).

In each of the experiments, 72-h forecasts were made from 0000GMT on 5 Feb., 10 Feb., 15 Feb., 20 Feb., and 25 Feb., and compared to control forecasts and the verifying states from the nature run. Comparisons were made in terms of growth of rms error in level 9 zonal wind speed (U_9), surface pressure (P_s), and level 5 (around 500 mb) zonal wind speed (U_5). In addition, subjective evaluation of isobaric sea level and upper level contour maps was performed for several cases.

Table 1 displays rms errors relative to <u>nature</u> in P_s and U_5 for individual forecasts from the control, PW-DIM, PW-SCM and PT-SCM initial states, with the statistics sorted by day and region. Statistics for U_9 and for other regions (Eurasia, North Atlantic, South America) were similarly prepared and studied. The errors for day 0 represent the errors in the initial states.

Table 1

Comparison of 3-Day Forecast Surface Pressure (Upper) and Level 5 Zonal Wind (Lower) Errors from Control (C), Perfect Wind (DIM and SCM), and Perfect Temperature Sounding (PT) Initial States

		5 FEBRUARY				10 FEBRUARY				15 FEBRUARY				20 FEBRUARY				25 FEBRUARY			
Region	Day	C	DIM	SCM	PT	C	DIM	SCM	PT	C	DIM	SCM	PT	C	DIM	SCM	PT	C	DIM	SCM	PT
Surface Pressure Error (mb)																					
Lat 30-86°	0	1.1	1.3	0.7	0.8	1.1	1.1	0.7	0.6	1.1	1.3	0.7	0.6	1.2	1.2	0.7	0.7	1.2	1.3	0.8	0.6
Lon 0-165°	1	2.8	3.0	2.1	2.8	2.3	2.3	2.5	2.2	1.8	1.7	1.4	1.2	1.8	1.5	1.3	1.3	3.5	2.8	2.3	2.1
Land	2	5.1	4.6	2.8	3.7	2.3	3.7	2.9	2.5	2.2	2.5	1.9	1.9	2.4	2.9	2.1	2.0	4.5	4.0	3.8	3.2
(N.America)	3	6.3	4.2	2.9	3.3	3.2	3.2	3.1	3.5	3.0	3.5	2.5	2.5	3.9	3.9	3.1	3.3	3.5	3.5	4.1	3.3
Lat 30-86°	0	1.4	1.8	1.0	1.7	1.2	1.8	1.0	1.0	1.2	1.8	0.9	0.9	1.5	1.7	1.0	0.9	1.2	1.4	1.0	0.9
Lon 275-60°	1	4.4	4.1	3.4	3.7	2.2	2.9	2.1	2.1	2.1	2.8	1.7	1.3	3.0	1.8	2.0	1.3	2.6	2.6	2.0	1.3
Water	2	4.6	5.3	3.7	4.0	2.7	3.7	2.8	3.0	3.2	2.8	2.4	2.0	3.1	3.0	2.9	2.0	3.3	3.0	3.1	1.7
(N.Pacific)	3	5.1	6.4	4.6	5.1	3.2	3.7	3.2	4.0	3.2	3.0	2.7	2.5	3.8	3.4	3.2	3.0	3.4	3.1	3.7	2.6
Lat -26-+26°	0	1.4	1.8	1.0	1.0	1.2	1.7	0.9	0.9	1.2	1.8	0.8	0.7	1.2	1.7	0.9	0.7	1.3	1.8	0.8	0.8
Lon 0-355°	1	2.5	2.2	1.7	1.5	1.9	2.1	1.4	1.4	1.9	1.9	1.3	1.2	2.0	2.2	1.4	1.2	1.9	1.7	1.2	1.1
Water	2	2.2	2.3	1.7	1.6	1.8	2.0	1.5	1.4	1.8	1.7	1.3	1.3	1.8	1.9	1.3	1.2	1.9	1.8	1.5	1.3
(Trop.Ocean)	3	2.3	2.2	1.7	2.2	1.9	2.2	1.7	1.5	1.7	1.7	1.5	1.4	1.7	1.7	1.4	1.3	1.9	1.7	1.5	1.5
Level 5 Zonal Wind Error (m/s)																					
Lat 30-86°	0	3.6	3.7	2.0	2.1	3.3	3.6	1.6	1.6	2.9	3.6	1.4	0.9	3.4	3.1	1.4	1.4	3.4	3.9	1.4	1.4
Lon 0-165°	1	4.7	4.0	3.0	2.9	4.1	4.7	3.8	3.5	3.5	3.5	1.9	1.4	3.7	3.9	2.2	2.2	4.7	4.4	3.6	2.4
Land	2	6.8	7.3	4.5	5.0	5.9	6.0	5.4	4.8	4.3	4.9	2.8	2.4	3.8	5.1	3.6	2.8	6.0	6.0	6.0	4.2
(N.America)	3	10.7	8.8	5.3	6.6	7.9	6.7	7.0	6.7	5.6	6.2	4.3	3.6	5.5	6.7	4.7	3.5	5.7	7.4	7.0	5.2
Lat 30-86°	0	8.2	8.1	5.6	6.5	4.5	5.8	3.4	2.7	5.4	4.5	2.5	1.6	5.4	5.5	2.6	1.5	5.5	5.2	3.9	1.6
Lon 275-60°	1	8.0	7.9	5.9	7.0	4.6	6.1	3.6	3.4	5.3	5.0	2.5	2.3	4.4	4.2	3.3	2.1	5.0	5.3	3.9	2.0
Water	2	7.2	6.9	6.8	7.3	5.8	5.6	3.9	3.8	5.2	4.6	3.3	2.7	4.7	4.9	4.2	3.2	5.5	6.1	4.5	2.0
(N. Pacific)	3	6.9	6.8	7.4	6.7	6.7	6.3	5.0	4.4	6.8	5.3	4.3	3.3	7.2	5.7	4.8	4.4	6.7	6.0	5.1	2.0
Lat -26-+26°	0	8.6	8.4	8.6	8.3	9.3	10.1	8.7	8.3	9.9	8.9	7.6	7.0	8.9	9.2	6.8	6.5	8.5	9.2	7.1	6.2
Lon 0-355°	1	9.6	9.7	9.5	8.3	9.5	9.7	8.7	8.0	9.5	9.3	8.0	7.3	9.2	9.7	7.3	6.6	9.3	9.1	7.7	6.3
Water	2	9.7	9.8	9.3	7.8	9.7	9.6	8.9	8.6	8.9	9.4	7.8	7.4	8.8	9.8	7.3	6.4	9.7	9.5	7.9	7.2
(Trop.Ocean)	3	10.2	9.9	9.7	8.9	9.8	9.8	9.1	8.9	9.2	10.1	8.3	8.1	9.7	9.9	7.8	7.2	9.6	9.2	8.1	7.7

Because of the small sample size, there was no attempt to establish the statistical significance of the average differences between the control and satellite forecast; however, as an example, the average growth of error is shown graphically in Fig. 1 for P_s so that relative differences in forecast errors can be assessed subjectively.

The results of the PW-DIM experiment generally confirmed the expectation that direct insertion of level 9 winds would have no significant impact on analyses and forecasts. The only significant response seen is about a 10% average improvement in the level 9 zonal (and meridional) wind component in the initial states over oceanic regions. However, errors in the initial sea level pressures suggest a tendency for the PW-DIM surface pressure field to be degraded slightly by the wind data assimilation, especially in the tropics. The isobaric analysis examined in the tropics, where mean gradients are weak, revealed that small scale variations had been added to the PW-DIM fields. The variations are probably associated with shock attending the DIM assimilation.

A comparison of forecast rms errors between Control and PW-DIM forecasts shows two interesting effects. Primarily, overall mean impacts are small in all variables and regions. The improvement in U_9 fields is usually lost with the first forecast day. However, subjective examination of sea level pressure charts did indicate a few noticeable impacts in individual forecasts, usually shown as improved placement and intensity of extratropical cyclones over oceanic areas.

The assimilation of error free level 9 winds by successive correction (PW-SCM) resulted in much larger and more consistent positive impacts on analyses and forecasts. Reductions of rms U_9 errors relative to the Control or PW-DIM analyses averaged about 30%. Initial surface pressure errors, which were larger than the Control for the PW-DIM analyses, are slightly lower than Control errors. The improvements in the U_9 and P_s analyses are consistent from region to region and from day to day (see Fig. 1). Average improvements in the U_5 PW-SCM fields are 30%, except over

Figure 1

PSFC AVERAGE FORECAST ERROR GROWTH CURVES

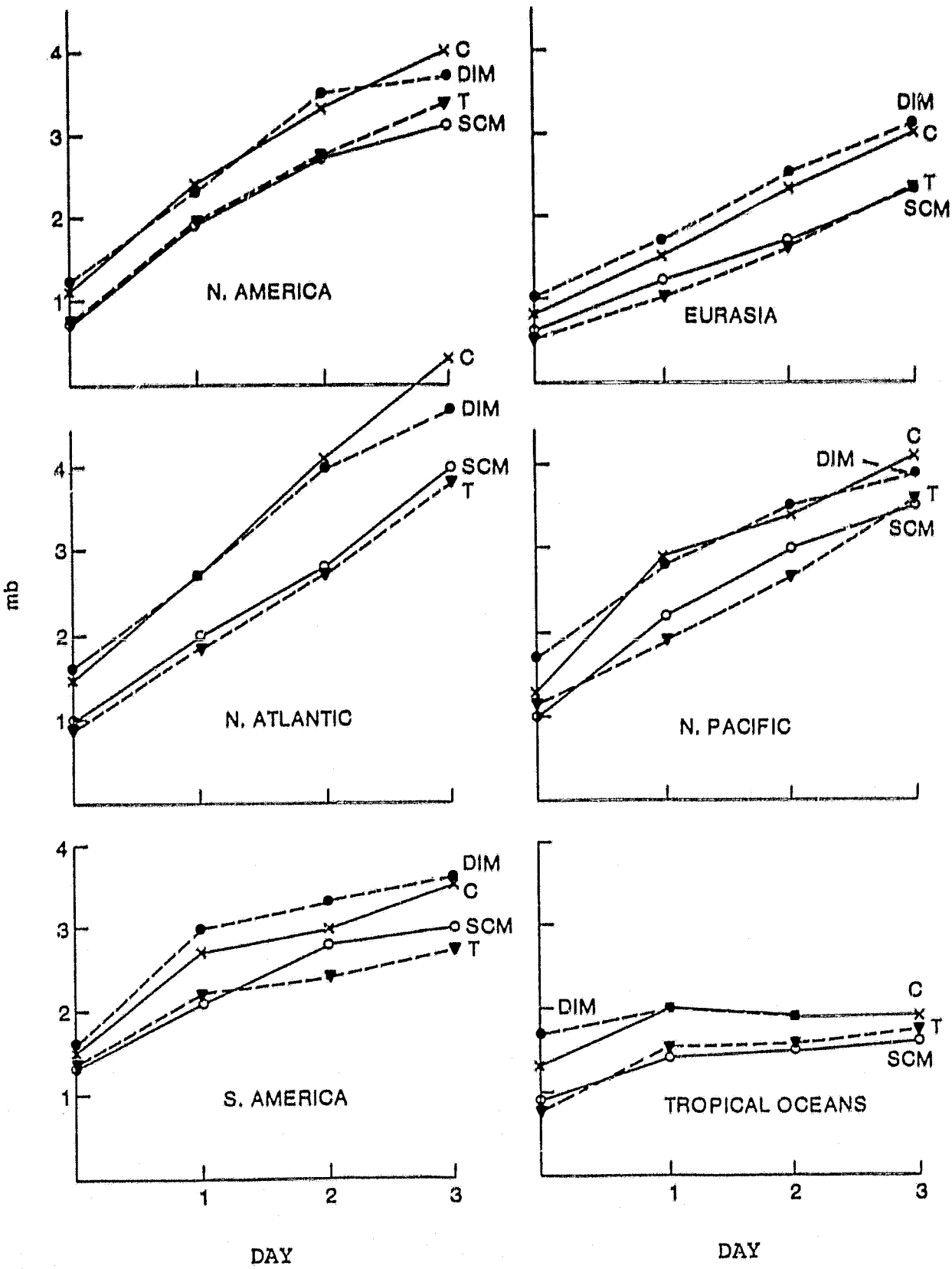

the tropical oceans and South America, where only slight impacts were found.

The forecasts made from error free wind SCM analyses are generally more skillful than corresponding Control and PW-DIM forecasts by margins equivalent to relative differences in the initial states. In contrast to the PW-DIM forecasts, which displayed occasional positive impacts, the forecasts of U_9 and P_s are improved over Control and DIM forecasts in all cases and all regions. On the other land, at level 5, improvements in the PW-SCM initial states did not always lead to improvements in the forecasts.

A subjective evaluation of the improvements showed that the predominant effect of the assimilation of SASS data was to greatly reduce the large and spatially coherent errors which characterized the control level 9 over ocean windfield. That improvement in turn led to substantial improvements in the 3 day forecast level 9 wind field and surface pressure field both over ocean areas and over downstream continental regions. It was apparent also that the impacts favored the eastern North Pacific Ocean, where Seasat SCM forecast pressure analyses revealed consistently better forecasts of the intensity and placement of extratropical cyclones. This feature of the simulations may be related to the poor coverate of conventional data in the North Pacific, relative to the North Atlantic and continental regions, and to the fact that the simulated Seasat orbit favored the insertion of simulated Seasat wind data over the Pacific during tne 6-h period prior to 0000 GMT, which was the initial time for all forecast simulations.

The PT-SCM experiment was conducted to provide an indication of the relative impact of surface wind data compared to sounder data, when both sets of observations could be considered to be error free. Most previous simulation studies have in fact dealt with sounders. While the earlier studies have tended to be quite optimistic regarding the potential impact of sounder derived temperatures on NWP, much of the optimism probably stemmed from unrealistic Control experiments and the assumption of sounder errors much lower than have been attained operationally. Recent

studies with real data, have shown that sounders can have small, but statistically significant positive impact on NWP. The impact appears to be highly sensitive to the quantity of data and the assimilation method. For Nimbus sounder data, assimilated time-continuously by SCM, Ghil et al. (1979) find 5-7% positive impacts in rms measures of forecast skill over North America.

The results of the simulated perfect Nimbus souding SCM experiment can be seen in Table 2 and Fig. 1. In general the impacts found were comparable to those of the PW-SCM experiment. The only difference evident is that the sounding data is slightly more effective than the surface wind data in controlling growth of level 5 forecast wind errors. Within the context of our experiment, the two data types appear to have equivalent value in reducing surface pressure errors. The perfect sounding produced about a 15% improvement in sea level pressure (rms) forecast errors. This appears to be a more reasonable upper limit to impacts to be expected from satellite data than have been predicted in less realistic OSSE's.

It is reasonable to assume that the idealized error free wind experiments overestimate the positive impact to be expected from real Seasat-1 data. However, a limited SCM experiment was performed to assess the effect of nominal errors on the satellite winds (±2m/s in speed, $\pm 20^{\circ}$ in direction, normally distributed). The results of that experiment are compared to the error free experiment in Fig. 2. Evidently for the fairly dense distribution of remotely sensed winds, the SCM assimilation is very effective at removing errors that are uncorrelated. Actual scatterometer wind data is likely to have a more complicated error structure, but may significantly impact forecasts if the errors are as small overall as the above, and if a good enough assimilation scheme is used.

A comparison of the PW-SCM and PT-SCM experiments suggests that surface wind data has the same potential impact as temperature sounders, when both sets of observations are error free, especially over the downstream of the eastern North Pacific and

Figure 2

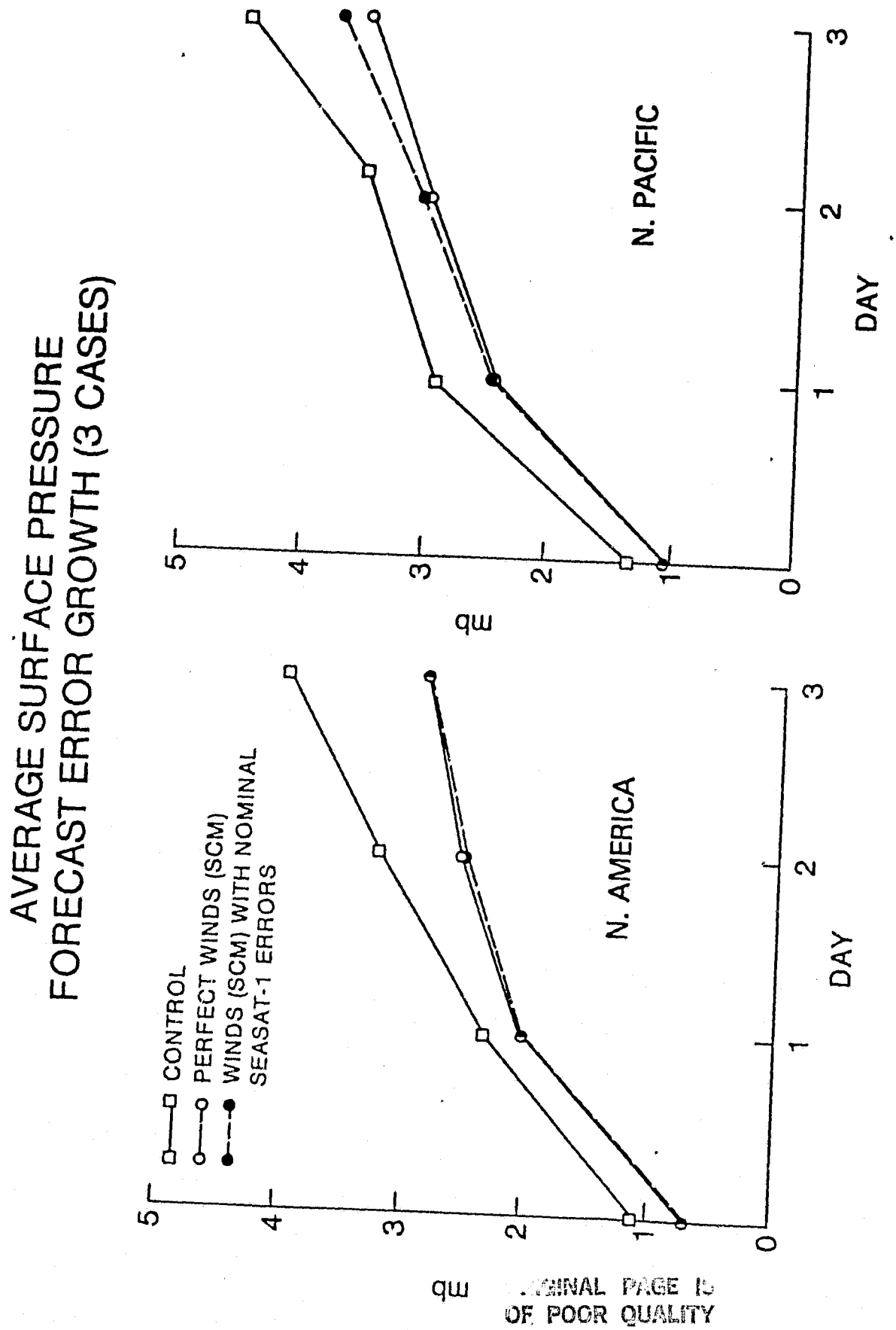

North Atlantic basins. Cane et al. (1979) contend that indirect support for this result is provided by Blackmon, et al. (1979). They show from observational data that over the eastern sides of the Northern Hemisphere oceans the 500 mb height is much more strongly correlated with 1000 mb height than with 1000-500 mb thickness and infer that surface (1000mb) data would play an important role in the determination of mid tropospheric structure. Satellite sounding data are of greatest potential over continents, where Blackmon et al. show that 500 mb height is more strongly correlated with 1000-500 thickness than with 1000 mb height. However, over continents, sounding data are largely redundant with conventional radiosondes.

The mechanism which Cane et al. (1979) hypothesize as responsible for the relatively large impacts of simulated Seasat data emerges as follows. Given the essentially barotropic nature of the atmosphere over the eastern North Pacific and North Atlantic, improvements in the surface (pressure) fields can significantly impact tropospheric analyses and forecasts. In terms of geostrophic adjustment theory, the scale of the wind data assimilated is small compared to the (barotropic) radius of deformation. Therefore it is reasonable to expect wind information to be retained and the mass field to adjust, while temperature data will tend to be radiated away as gravity waves. Further, from a statistical point of view, there is more information in a small orbit segment of wind data than in sounder data of the same size because the correlation scale of winds is smaller. This suggests that wind data can benefit more from the dense coverage that a satellite provides. In addition, even the preliminary evaluation of actual SASS data suggests that scatterometer wind errors are a smaller fraction of marine boundary layer wind analysis error than are sounder temperature errors compared to temperature analysis.

The results of these idealized impact studies, coupled with the fact that actual Seasat-A SASS marine wind data have an accuracy close to nominal specifications suggest that studies involving real SASS global data sets should be undertaken and that serious consideration be given to such data in the design of an optimum global observing system.

3. FUNCTIONAL DESCRIPTION AND DOCUMENTATION OF GMSF GLOBAL SPECTRAL OCEAN WAVE MODEL (GSOWM)

To implement a global spectral ocean wave model (hereafter GSOWM) usable on the Amdahl 470 at Goddard Modelling and Simulation Facility (hereafter GMSF) and readily portable to any IBM 370 of roughly the same size, three programs were written and tested. Programs PRELIM (to print grid coordinates and propagate tables, and write propagate tables to disk) and ICEDECK (to write land-sea tables to disk) need be run once each, at installation time; program PAXXPAXX contains the growth and propagation modules, and is run for every time segment it is proposed to simulate.

The auxiliary programs DUMP13, DUMQ13, DUMP14 permit retrieval of the records written to the output datasets by PAXXPAXX.

3.1 PRELIMS. This program, for computing propagation coefficients on a truncated latitude-longitude grid (the polar caps are deleted), derives from a program submitted to FNWC in 1977 for a full latitude-longitude grid (including the poles) with improvements discovered while adapting the program to a transverse Mercator grid for NOAA/AOML/SAIL in 1978. The principal novelty introduced in 1978 was the uniform use of a triangle on the earth as a basis for computing the outbound propagate table: in 1977 rectangles were used in general, but triangles where the longitudinal spacing changed. The principal novelty introduced here is the use of a distinct scratch file for each propagable frequency (14 in the model submitted: see §3.1.1) which remarkably simplifies the housekeeping operations in transposing the propagate table (§3.1.5.7).

3.1.1 Data definitions

13 Dataset containing the transposed propagate table: 79 tracks. This dataset is referenced every time a wave field is simulated; if disk storage is labile, a backup tape is advisable.

15 through 28. Datasets containing the inbound propagate tables for the 14 propagable frequencies: 6 tracks each. After successful execution of PRELIMS, these can be decatalogued.

3.1.2 Grid numbering system.

Grid points are numbered by the subscripts (LONG,LAT), $1 \le LONG \le 76$, $1 \le LAT \le 73$. LONG increases from west to east; LAT increases from south to north. Grid points may also be referenced by the single subscript KPOINT = LONG+76*(LAT-1). Denote true latitude (degrees, north positive) by ALAT; true longitude (degrees, east positive) by ALONG. Then

ALAT = -74.0+4.0*LAT,

ALONG = AMOD(80.0+2.5*MOD(LAT,2)+5.0*LONG,360.0)-180.0.

On the globe, points with ALONG = 73, 74, 75, 76 over i.e. points with ALONG = 1, 2, 3, 4. This unusual choice of prime meridian obviates a coding exception to prevent waves from propagating across the Isthmus of Panama: the land-sea table handles the exception.

3.1.3 Input parameters.

In the program as submitted there are none. In a generalized program accommodating arbitrary numbers of frequency and direction bands, the numbers 14 and 20 occurring in DIMENSION statements would be PARAMETER variables; the variables FREQ1 and FREQ2 would be input parameters. Then compute WEDGE as 180 divided by the number of directions; compute RAT = (FREQ2/FREQ1)**(1./(NF-1.5)), where NF is the number of frequencies; compute DELT as discussed in §3.1.5.4.

3.1.4 Common blocks.

N.B. All variables in blank common are local and volatile.

```
 COMMON
$/YPARAM/ LLAT,LLONG,LPNT1,LPNT2,FREQ(14),FREQ1,FREQ2,SPACE(2)
$  ,WEDGE,DIREC(20),DELT
$/YSHORT/ TLAT(3,73),TLONG(2,76)
$/YYOUTB/ JTABLE,TABLE(4,20,73)
$/YYTRIG/ DLAT,COSS,DANGLE,CLAT,TRAVEL,RAD,CTR,STR,
$  OMIN,017,RAT(3,73)
```

YPARAM:

LLAT number of parallels, i.e. 73

LLONG number of meridians, i.e. 76

LPNT1 number of grid points, without deduction for land, but with duplicates excluded: 73×72 = 5256

LPNT2 gross number of grid points: 73×76 = 5548

FREQ nominal frequencies of the 14 bands

FREQ1 nominal frequency of lowest band, i.e. .04 hertz

FREQ2 nominal frequency of highest band, i.e. .20 hertz

SPACE approximate maximum and minimum values of grid spacing,nm

WEDGE half of the angular bandwidth, i.e. 9°

DIREC array of 20 directional bands, in degrees, clockwise from north: DIREC(I) = 18*I-9. Note: in 1977 we found that propagation along a meridian or the equator entailed a vexatious exception to the general code; directional bands are now chosen to miss the cardinal points.

DELT time step used in propagation, i.e. 3 hours. See §3.1.5.3.

YSHORT:

TLAT functions of grid latitude. See §3.1.5.2.

TLONG functions of grid longitude. See §3.1.5.2.

YYOUTB:

JTABLE grid point numbers and angular band numbers in outbound propagation table. See §3.1.5.5.

TABLE energy fractions in outbound propagation table. See §3.1.5.5.

YYTRIG:

DLAT colatitudes, in radians

COSS cosines of the 20 directions

DANGLE the 20 directions, in radians, reduced to the range $(-\pi, +\pi)$

CLAT cosines and sines of the colatitudes

TRAVEL distance covered by waves of each frequency, at their group velocity, in time DELT, in nm. See §3.1.5.4.

RAD $180/\pi$

CTR cosines of TRAVEL

STR sines of TRAVEL

OMIN $\pi/10800$

017 $\pi/180$

RAT correction factors for convergence of meridians. See §3.1.5.4.

3.1.5 Subprograms.

3.1.5.1 MAIN. Defines common blocks, calls GGRID, BANDS, and TRIG (once each), calls OUTBND followed by INBND (once for each frequency), calls TRANSP once, and writes a file mark on dataset 13. (This step was inserted when coding for SAIL, where all permanent files are tapes).

3.1.5.2 GGRID. The principal products of the program are arrays TLAT (referenced by subroutine TRIG), and JLAT, JLONG, ALAT, ALONG (used to print table of coordinates). JLAT, JLONG, ALAT, ALONG become obvious upon inspection of the printed output; TLAT, TLONG require explanation. TLONG(1,I) is the true longitude of the grid points (I,1), (I,3), etc.; TLONG (2,I), of the points (I,2), (I,4), etc. To understand TLAT, draw the 73 parallels, as well as zigzag lines connecting grid points on adjacent parallels, yielding a mesh of isosceles triangles: the point (ALAT, ALONG) has the 6 neighbors (ALAT, ALONG±5), (ALAT±2, ALONG±2.5).
TLAT (1,I) true latitude corresponding to grid latitude I.
TLAT (2,I) base of isosceles triangles, i.e. 5° of longitude, in nm.
TLAT (3,I) approximate mean value (flat earth computation) of legs of isosceles triangles.

3.1.5.3 BANDS. Computes the midpoints of the 20 angular bands and the nominal frequencies of the 14 frequency bands. The choice of frequency-direction bands (or bins) for a SOWM has been more arbitrary than scientific. Uji & Isozaki have used bands uniformly spaced in period. Pierson in principle uses elementary bands of width 1/180 hertz (to agree with an ancient Tukey spectral

analysis of wave records at British weather ships); at higher frequencies, he groups 2, 3, or 4 elementary bands into one working band. If wave spectra are approximately similar, then spectral resolution is equalized at all sea states by spacing the frequencies in geometric progression. A little trial showed that a ratio of 5 between the highest and lowest bands was adequate, but that the absolute frequency of the lowest band may need to be shifted according to the wave regime under study. The desirable number of angular bands is also uncertain. Gelci in his early experiments used 8 bins. Pierson et al. prepared a 12-angular-band model for FNWC, and concluded from their numerical tests that 24 bands would yield much better representation of swells. We used 24 bands in the limited-area SOWM prepared for SAIL. If the purpose of banding is a faithful modelling of propagation, then the termini of group-velocity vectors corresponding to a frequency-direction band should approximate the vertices of a square, leading to an angular bandwidth (in radians) of $\log_e (\omega_{i+1}/\omega_i)$.

With the value of RAT used in BANDS, the angular bandwidth would be 7.38°: in round numbers 7.5°, or 48 bands. We are aware of no numerical experiments with angular resolution this fine, perhaps because very few series of directional spectra have been acquired to calibrate such a model.

3.1.5.4 TRIG. Computes the great-circle distance traveled in one time step at each nominal frequency, and trigonometric functions of these arcs, colatitudes, and directions of propagation. These calculations are in double precision because we will be solving an ill-conditional spherical triangle: two long sides (colatitudes of origin and terminus of propagation vector) and one short side (distance traveled, which is less

than 2°.) The time step DELT is chosen as the largest multiple of 1 hour in which the .04 hertz waves travel less than 120 nm. TRIG also computes the area ratio between adjacent parallels: each grid point is treated as a box 120 nm × (300 cos ALAT) nm, and the quantity conserved in propagation is the wave variance multiplied by the area of the box.

3.1.5.5 OUTBND. Executes steps 1, 2, 3 of §3.1.6. The numbering of the eight quadrant indicators is:

KWAD2 = 0. LAT is even and wave moves NE
KWAD2 = 1. LAT is even and wave moves NW
KWAD2 = 2. LAT is even and wave moves SE
KWAD2 = 3. LAT is even and wave moves SW
KWAD2 = 4. LAT is odd and wave moves NE
KWAD2 = 5. LAT is odd and wave moves NW
KWAD2 = 6. LAT is odd and wave moves SE
KWAD2 = 7. LAT is odd and wave moves SW

The numbering of the four triangles is:

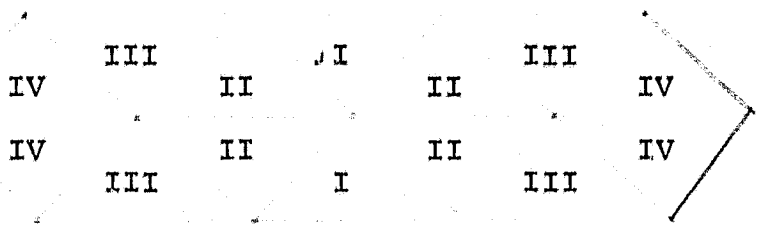

Triangles III and IV occur only at latitudes greater than $\pm 66^{\circ}$ and frequencies of .04 and .045496 hertz. In numbering the vertices of the triangles, the upper sign affixed to ALAT applies to the NE and NW quadrants; the upper sign affixed to ALONG applies to the NE and SE quadrants. Waves start at the point (ALAT, ALONG).

Triangle I, vertex 1: ALAT ±2.0, ALONG ±2.5
2: ALAT ±2.0, ALONG ∓2.5
3: ALAT, ALONG
Triangle II, vertex 1: ALAT, ALONG ±5.0
2: ALAT ±2.0, ALONG ±2.5
3: ALAT, ALONG

Triangle III, vertex 1: ALAT ±2.0, ALONG ±7.5
2: ALAT, ALONG ±5.0
3: ALAT ±2.0, ALONG ±2.5
Triangle IV, vertex 1: ALAT, ALONG ±10.0
2: ALAT ±2.0, ALONG ±7.5
3: ALAT, ALONG ±5.0

3.1.5.6 INBND. Executes step 4 of §3.1.6.

3.1.5.7 TRANSP. Executes step 5 of §3.1.6. In order to economize storage by using the type INTEGER*2, the present code differs from previous transpose routines in that the arrays JTAB4 and TAB4 are not equivalenced. Contents of JTAB4 and TAB4:

IFR indexes frequency
IDIR indexes direction
LAT is grid latitude
JTAB4(1,IFR,IDIR,LAT) is an integer in the range 1 to 6 (on the average 4): the number of parts in the propagation formula.
JTAB4(2*J,IFR,IDIR,LAT) is the transmitting grid point number minus the receiving grid point number. Used to enter the land-sea table and verify that the transmitting grid point is water before propagating.
JTAB4(2*J+1,IFR,IDIR,LAT) is the relative address of the transmitting band from the receiving band, biased by -21280.
TAB4(J,IFR,IDIR,LAT) is the fraction of energy in the transmitting band to be moved to the receiving band.

3.1.6 Construction of propagate table.

1. Start a unit component (one direction-frequency band), multiplied by the area of a rectangle centered on a grid point, and propagate it from that point at its proper group velocity and along an arc of a great circle for a time step. In

general the receiving point will be in the interior of a triangle bounded by grid points, and the true azimuth at the receiving point will not be one of the 20 azimuths used in CMPE27.

2. Propagate a suitable fraction of energy into each of the 3 grid points, corners of that triangle. Turn a fraction of one of those fractions through $\pm 15^{\circ}$ (toward the equator) to conserve the mean azimuth at the receiving point. The search for a fraction to turn is made over vertices 1, 2, 3 in order.
3. Divide each of the 4 energies found in (2), which sum exactly to the energy transmitted in (1), by the area of the rectangle centered on the receiving grid point, thus reconverting them to spectral components.
4. The result of step (3) is an outbound propagation matrix, which tells where the energy at time step N goes at step N+1. It is now necessary to transpose this matrix, yielding an inbound propagation matrix containing the multipliers to be applied to the several transmitting grid points and directional bands at time step N-1 to obtain one band at one receiving grid point at step N. The number of multipliers averages 4: it varies from 1 to 6, in the model submitted. The numbers 0 and 7 have occurred with other grids.
5. The result of step (4) is an inbound propagation matrix for each latitude and each propagable frequency: a further transposition brings together the coefficients for each latitude, yielding the propagate tables JTAB4 and TAB4.

3.2 ICEDECK. Turns the data statement (written for convenience in punching) into a printed land-sea table and an array stored in DD11. The convention is 1 = land, 2 = sea.

3.3 PAXXPAXX.

3.3.1 Data definitions

10 Dataset containing the wind field, at 4-hour intervals: 3½ tracks per field. The length of a logical record is 11096 words, dimensioned (2,76,73).

Word (1,LONG,LAT) contains wind speed, m/sec, at the grid point (LONG,LAT).
Word (2,LONG,LAT) contains wind direction, to which the wind is blowing, in degrees, clockwise from south.

11 Dataset containing the land-sea table written by ICEDECK. 1 track.

12 Dataset containing the propagate table, i.e. DD13 written by TRANSP (§3.1.5.7) 79 tracks.

13 Principal output file (tape): 3.13 megabytes for each time step declared by KSTEP3. For format of records see §3.3.3.

14 Supplementary output file (disk): 2 tracks per time step. For format of records see §3.3.3.

17 Scratch file (disk): 241 tracks.

18 Scratch file (disk): 241 tracks.

3.3.2 Input parameters (in namelist $WHAT).

```
 NAMELIST /WHAT/ LWIND,LLAND,LPROP,LOUT,LARCH1,LARCH2,
$  LRST1,LRST2,LSCR1,LSCR2,KSTEP1,KSTEP2,KSTEP3,YMDH,LSKIP,KBT,
$  CA,CB,RUNID
```

N.B. The parameters LWIND, LLAND, LPROP, LOUT, LARCH1, LARCH2, LRST1, LRST2, LSCR1, LSCR2, were included in case the default values of DDs should be unavailable at an installation. Do not use them.

KSTEP1 Number of first time step. For dead start, KSTEP1 = 1; to continue a previous simulation, KSTEP1 (new run) = KSTEP2 (previous run) + 1.

KSTEP2 Number of last time step. The length of a simulation is (KSTEP2-KSTEP1+1) steps, i.e. 3*(KSTEP2-KSTEP1+1) hours.

KSTEP3 Frequency of full output. The tape LARCH1 is written when MOD(ISTEP,KSTEP3) = 0. Plausible values for KSTEP3 are 2,4,8; these archive wave spectra every 6,12,24 hours.

YMDH Date and time corresponding to ISTEP = 0, supplied as an 8-digit integer YYMMDDHH: for example, 79092511.

LSKIP Number of logical records on DD10 to be skipped before reading the first wind field wanted. (default = 0).

KBT The default value, KBT = 1, produces a hump (as used by Inoue at $\omega U_* \cos\theta/g = .031$; to remove the hump, set KBT = 0.

CA The multiplicative constant in the linear growth mechanism. The default value is 1.36E-9; any alternative value (for sensitivity studies) must be in the deck $WHAT.

CB The multiplicative constant in the exponential growth mechanism. The default value is .1066; the value .0231 is believed to be physically correct.

RUNID A 9-digit integer serving as a mnemonic to identify a simulation run.

3.3.3 Format of output data sets.

DD13: each time step writes 147 logical records followed by a file mark. Logical record 1 contains 3 words, INTEGER*4, of identification: the time step, the current date and time, and the run ID. Logical record (2*LAT) contains 76 words, REAL*4, the largest energy (wave variance, m^2) in one band at the point (LONG,LAT). Words 1, 2, 75, 76 are meaningless. Logical record (2*LAT+1) contains 21280 words, INTEGER*2, representing an array dimensioned (14,20,76). Word (IFREQ,IDIR,LONG) contains the variance (m^2) in the spectral band (IFREQ,IDIR) at the point (LONG,LAT), divided by the largest variance in any band at that point, scaled by $2^{15}-1$, rounded and converted to integer.

DD14: each time step writes one logical record, containing 4 words, INTEGER*4, of identification (array JFRONT) followed by 5548 words, REAL*4, dimensioned (76,73), containing the significant height, in meters, at the point (LONG,LAT).
N.B.: when JFRONT(4) = 0, a full spectral record is written to DD13.

DD18: same format as DD13, but no file mark. Before continuing a simulation, copy DD18 to a backup (disk or tape).

3.3.4 Common blocks

```
 COMMON
$/XXXXIO/ LWIND,LLAND,LPROP,LOUT,LARCH1,LARCH2,LRST1,LRST2,
$  LSCR1,LSCR2,RUNID
$/XXTIME/ KSTEP1,KSTEP2,KSTEP3,ISTEP,DELT,DELTAH,YMDH,ZMDH,
$  LSKIP,KBT
$/XSPEC1/ SPOLD(280,76,3)
$/XSPEC2/ SPNEW(280,76)
$/XPARAM/ CA,CB,FREQ1,FREQ2,WEDGE,DIREC(20),COSS(2,10),
$  DELOG,OMEGA(2,14),FREQ(14),DOM(14),RBW(14),OMM4(14),
$  OM3DD(14),OM116(14),OM25(14),DOMM4(14),OMK(14)
$/XXGRID/ LAT,LONG,KPOINT
$/XXLAND/ LANSEA(76,73)
$/XXWIND/ WIND(2,76,73)
$/XXXH13/ FRONT(4),H13(76,73)
$/XXPROP/ JPROP(13,280,73),PROP(6,280,73)
$/XXPACK/ EEE(76),SPEC16(280,76)
```

3.3.4.1 XXXXIO

LWIND = 10

LLAND = 11

LPROP = 12

LOUT = 6

LARCH1 = 13

LARCH2 = 14

LRST1 = 15. Not used.

LRST2 = 16. Not used.

LSCR1 = 17

LSCR2 = 18

RUNID See §3.3.2.

3.3.4.2 XXTIME

KSTEP1, KSTEP2, KSTEP3, YMDH, LSKIP, KBT See §3.3.2.

DELT: the growth time step (½ the propagation time step) in seconds. i.e. 5400 seconds.

DELTAH: the propagation step in hours, i.e. 3 hours.

ISTEP: a do-loop index, running from KSTEP1 to KSTEP2.

ZMDH: current value of date and time, in same format as YMDH (see §3.3.2). At time ISTEP = 0, ZMDH is set equal to YMDH; at each subsequent time step, ZMDH is updated by adding DELTAH and reducing as necessary modulo 24 hours, 28,29,30,31 days, 12 months, and 100 years.

3.3.4.3 XSPEC1

SPOLD The spectra before propagation, at the three parallels LAT, LAT±1.

3.3.4.4 XSPEC2

SPNEW The spectra at the parallel currently being computed.

3.3.4.5 XPARAM

CA,CB See §3.3.2.

FREQ1,FREQ2,WEDGE,DIREC See §3.1.4.

COSS Array of cosines and sines of multiples of 18°.

DELOG = ALOG(FREQ2/FREQ1)/12.5, i.e. the ratio between frequencies of successive bands.

OMEGA Array of radian frequencies. OMEGA(1,I) is the lower limit of band I; OMEGA(2,I) is the nominal frequency.

FREQ Array of nominal frequencies, in hertz.

DOM Array of bandwidths, in radians/sec.

RBW Array of reciprocal bandwidths, in sec.

OMM4 Array of ω^{-4}

OM3DD The factor $C_{\alpha}\omega^{3}\Delta\omega\Delta\theta$ in the numerator of e.g. (5) of the growth documentation.

OM116 Array of $\omega^{1.16}$, used in approximate computation of resonant wave number. See eg. (9) of §3.3.7.

OM25 Array of $\omega^{-2.5}$, used in computing the exponent s in Miysuyasu's spreading function. See eg. (17) of §3.3.7.

DOMM4 Array of $\omega_i^{-4} - \omega_{i-1}^{-4}$. Used in cutting back high frequencies. Step 13 of §3.3.7.

OMK Array of wave numbers ω^{2}/g.

3.3.4.6 XXGRID

LAT coded latitude of current grid point.

LONG coded longitude of current grid point.

KPOINT 76*LAT+LONG. Used in addressing land-sea table.

3.3.4.7 XXLAND

LANSEA See §3.2.

3.3.4.8 XXWIND

WIND See DD10 in §3.3.1.

3.3.4.9 XXXH13

JFRONT, H13 See DD14 in §3.3.3.

3.3.5.0 XXPROP

JPROP See account of JTAB4 in §3.1.5.7.

PROP See account of TAB4 in §3.1.5.7.

3.3.5.1 XXPACK

EEE, SPEC16 See DD13 in §3.3.3.

3.3.6 Subprograms

3.3.6.1 MAIN. Declares common blocks and calls WWORK.

3.3.6.2 Subroutines called once only

3.3.6.2.1 WWORK. Validates input, calls LODTAB, acquires an initial wind field, and sets up a do-loop to control growth, propagation, and output cycles.

Called by: MAIN

Calls: LODTAB,WWAX1,BUMP,QRWAX2, and utilities.

Method:

1. Set default values of parameters (ISN 7 to 30).
2. Read and echo namelist $WHAT (31-32).
3. Validate input (33-165).
4. Acquire land-sea table (166-167).
5. Acquire initial wind field (168-173). This wind field is used once only, in the first call to WWAX1. See §3.3.7.1.
6. Set ZMDH to the value corresponding to KSTEP1-1, calling BUMP if KSTEP1 > 1 (174-179).
7. Call LODTAB (180).
8. Acquire the tables JPROP and PROP (181-184). N.B. In this SOWM the entire propagate table is treated as resident; in models written for smaller machines, the table was read in, repeatedly, one parallel at a time.
9. Within do-loop in ISTEP, call WWAX1,BUMP, and QRWAX2 (185-190).

3.3.6.2.2 LODTAB. Computes the functions of direction and frequency contained in common block XPARAM.
Called by: WWORK

3.3.6.3 Subroutines called at every time step.

3.3.6.3.1 BUMP. Updates the year, month, day and hour shown in ZMDH by adding the hours in DELTAH, and, if necessary, adjusts the result by adding 1 day and subtracting 24 hours (ISN7); adding 1 month and subtracting 28, 29, 30 or 31 days (9-18); adding 1 year and subtracting 12 months (18, when MONTH = 12); subtracting 100 years (19-20).
Called by: WWORK

3.3.6.3.2 WWAX1. Reads wave spectra from DD17, applies half a time step (5400 seconds) of growth, and writes spectra to DD18. The code at ISN28-35 copies spectra onto the east and west margins of the cut cylinder, where they are expected by the propagate routine. For the sequence of wind field acquisition in WWAX1 see §3.3.7.1.
Called by: WWORK
Calls: UNPAQQ,CMPE27,PAQQ, and utilities.

3.3.6.3.3 QRWAX2. Reads wave spectra to DD18, unpacks them into array SPOLD, propagates to find the new spectra for one parallel and puts them in array SPNEW, applies half a time step of growth, writes the spectra at selected time steps to DD13, and writes the spectra at all time steps to DD17. The mathematical method is discussed in §3.3.8. The array MOOD, where MOOD(I) = MOD(I+1,3)+1, is introduced to save computing.
Called by: WWORK
Calls: GRAB,CMPE27,PAQQ and utilities.
Method:

1. Set up array (ISN7-10).
2. At selected time steps, write ID to DD13 (11).
3. Rewind DD17 and DD18 (13-14).

4. Acquire wind field (15). See §3.3.7.1.
5. Zero the significant height field (16-18).
6. Acquire two parallels of old spectra (19-20).
7. In a do-loop on LAT: (21).
8. If LAT < 72, acquire one parallel of old spectra (23-24).
9. Zero array of new spectra (25-27).
10. In a do-loop on LONG: (28).
11. If the point is land, get out (29).
12. Propagate. In order to follow the action at ISN32-42, it is advisable to compare each of the 2*KPART+1 references to array JPROP and the KPART references to array PROP with the corresponding values printed in subroutine TRANSP (§3.1.5.7.)
13. Call CMPE27 to effect the second half step of growth (45).
14. Compute significant height (46-50). Here endeth the loop on LONG.
15. At selected time steps, write spectra to DD13 (55-56).
16. At all time steps, write spectra to DD17 (57-58). Here endeth the loop on LAT.
17. Write significant height field to DD14 (60).
18. At selected time steps, write file mark on DD13 (61).
19. Print significant height field (63).

3.3.6.3.4 CMPE27. Takes a spectrum and applies growth and dissipation for the time step DELT contained in common block XXTIME. Note, that as used in this SOWM, DELT is half a propagation step, i.e. 5400 seconds.

Called by: WWAX1, QRWAX2

Data: UXMULT(I) = $\frac{u*}{U_{19}}$, where U_{19} = (I+2.11) m/sec.

UKAPPA(I) = $U_{19}\kappa_1$, where U_{19} = (I+2.11) m/sec,

and κ_1 is defined in eq. (9) of §3.3.7.

GAMMAK(I) = $.41\kappa^{0.28}$, where $\kappa = .01*(I+1)$.

DELTAK(I) = $.61543298\kappa^{-0.0528}$, where $\kappa = .01*(I+1)$.

These arrays are used to approximate the non-linear functions $u*(U_{19})$, $\kappa_1(u*)$, $\gamma(\kappa)$, $\delta(\kappa)$ by table look-up and interpolation: see ISN24-28, 159-160.

The steps below are keyed to §3.3.7.2:

1. not specifically modeled
2. (ISN16-17)
3. (24,27)
4. (25,28)
5. not used
6. (35-61)
7. (62-63)
8. (64-67)
9. (72-112)
10. (113)
11 (114-115)
12. (117-120)
13. (122-128)
14. (140-138)
15. (139-145)
16. (148-185)
17. (187-211)
18. (121, 212-216)

3.3.6.4 Packing and unpacking routines

These subroutines were not part of the SOWM as first written: they were added so that DD17 and DD18 could each fit in 241 tracks. At such time as 478 tracks each are available for DD17 and DD18, some CPU time can be saved by reverting to subroutines WORK, WAX1, PRWAX2.

3.3.6.4.1 PAQQ. Converts the spectrum at 76 grid points (85120 bytes) into 42864 bytes and stores them in arrays EEE and SPEC16 in the format sketched for DD13 in §3.3.3.

Called by: WWAX1, QRWAX2

3.3.6.4.2 UNPAQQ. Reverses the operation performed by PAQQ.
Called by: WWAX1, GRAB

3.3.6.4.3 GRAB. Reads 85120 bytes from DD18, calls UNPAQQ to unpack the spectra into SPNEW, and then moves them to the addresses in SPOLD controlled by the parameter I.
Called by: QRWAX2
Calls: UNPAQQ and utilities

3.3.6.5 Utility routines

The purpose of these 6 subroutines is to segregate I/O and related statements, thus minimizing the work needed to replace, if desired, FORTRAN reads, writes, rewinds, and file marks by calls to non-standard routines.

3.3.6.5.1 BREAD2. Reads NPOINT 2-byte words from LU to ARRAY.

3.3.6.5.2 BREAD4. Reads NPOINT 4-byte words from LU to ARRAY.

3.3.6.5.3 BRITE2. Writes NPOINT 2-byte words to LU from ARRAY.

3.3.6.5.4 BRITE4. Writes NPOINT 4-byte words to LU from ARRAY.

3.3.6.5.5 BEND. Writes a file mark on LU.

3.3.6.5.6 BREW. Rewinds LU.

3.3.7 The spectral growth and dissipation algorithm.

The growth model used is the linear model

$$dT/dt = A+BT \tag{1}$$

where $T = S\Delta\omega\Delta\theta$ is the spectrum integrated over one of the (NDIREC×NFREQ) = 280 computational bands. Growth is controlled by not permitting T to grow above

$$T_0 = M(\bar{\omega},\theta)\{\tfrac{1}{4}\alpha g^2 \omega_0^{-4}[\exp(-\omega_0^4/\omega_2^4)-\exp(-\omega_0^4/\omega_1^4)]\} \tag{2}$$

where $M(\bar{\omega},\theta)$ is an angular spreading function derived from Mitsuyasu et al. (1975); the expression in {} is a Pierson-Moskowitz spectrum; $\omega_1 < \omega_2$ are the limits of a frequency band, and $\bar{\omega} = \sqrt{(\omega_1\omega_2)}$. As formulated, $A/(\Delta\omega\Delta\theta)$ is a function of $\bar{\omega}$, θ, and u_* (the friction velocity); B is a function of the same arguments expressed as

$$B = \bar{\omega}B^*(\bar{\omega}u_* \cos\theta / g); \tag{3}$$

ω_0 is a function of U, the wind speed at 19.5 meters,

$$\omega_0 = \beta^{\frac{1}{4}} g/U; \tag{4}$$

α is a function of ε, the ratio of total energy to Pierson-Moskowitz energy, $\varepsilon = E/(\tfrac{1}{4}\alpha_0\beta^{-1}g^{-2}U^4)$; M is a function of θ & $\bar{\omega}/\omega_0$. We consider each of A, B, ω_0, α, M in turn.

A-term. Following Snyder & Cox (1966) and Inoue (1967, p. 12) we write

$$A = \frac{C_a u_*^4 \omega^3 \Delta\omega\Delta\theta}{[\gamma+(k\cos\theta-\kappa)^2/\gamma][\delta+k^2\sin^2\theta/\delta]} \tag{5}$$

where $k = \omega^2/g$, $\gamma = \mathrm{MAX}(.41\kappa^{1.28}, .0027422197)$, $\delta = \gamma^{.74}/.84$, & $\kappa = \omega/u_c$. The determination of u_c is the principal difficulty in applying (5) to wave growth. Inoue (1967, p. 22; $u^{2.25}$ is a computation slip for $u^{1.75}$) took u_c as the anemometer wind at 19.5 m.

According to Priestley (1965, p. 45) u_c is the wind at a height z of 5.3 wavelengths, i.e.

$$z = \frac{2\pi}{5.3\kappa} = \frac{2\pi u_c}{5.3\omega} . \tag{6}$$

To routinely solve the non-linear equation

$$\frac{\omega}{\kappa} = 2.5\, u_* \log \frac{2\pi}{5.3\kappa z_0}$$

for κ as a function of ω and u_* is awkward, and the following device was adopted, based on locally replacing a logarithmic profile by a power-law profile:

Take a reference height

$$\tilde{z} = 637.39 u_*^2/g$$

and compute

$$\begin{cases} \tilde{\kappa} = 2\pi/5.3\tilde{z}, \\ z_0 = .00001525 m^2 sec^{-1} u_*^{-1} + .001468 m^{-1} sec^2 u_*^2 - .0000371 m, \\ \tilde{u} = 2.5 u_* \log(\tilde{z}/z_0), \\ \tilde{\omega} = \tilde{\kappa}\tilde{u}. \end{cases} \tag{7}$$

For $u_* = 1$ m/sec, corresponding to $U_{19.5} = 23.773$ m/sec, this calculation yields

$$\tilde{z} = 65.0 \text{ m}$$
$$\tilde{\kappa} = .018238564 \text{ m}^{-1}$$
$$z_0 = .00144615 \text{m}$$
$$\tilde{u} = 26.783094 \text{ m/sec}$$
$$\tilde{\omega} = .48848518 \text{ sec}^{-1} \text{ or } .0774483 \text{ hz.}$$

So far there is no approximation; to convert to other values of ω we introduce the scaling law

$$z/\tilde{z} = (u/\tilde{u})^{7.25} . \tag{8}$$

Substituting (8) in (6) yields

$$(u/\tilde{u})^{7.25} = (\kappa/\tilde{\kappa})^{-1} = (u/\tilde{u})(\omega/\tilde{\omega})^{-1}$$

so that

$$u/\tilde{u} = (\omega/\tilde{\omega})^{-0.16}$$

$$\kappa = \tilde{\kappa}(\omega/\tilde{\omega})^{1.16} = \kappa_1(u_*) \times \kappa_2(\omega) ,$$

where

$$\kappa_1 = \tilde{\kappa}\omega^{-1.16} \quad \& \quad \kappa_2 = \omega^{1.16}. \tag{9}$$

The constant C_a was chosen by fitting the absolute power density scaling factor of Priestley (1965, p. 51) to u_*, assuming a u_*^4 law and roughness parameter z_0 of .03 m corresponding to mowed grass) for the conditions of Priestley's experiment. The product of the fitted constant and all physical constants appearing in the relation between A and the pressure spectrum is $C_a = 1.36\times10^{-9}$ for A in m^2 and t in sec.

B-term. Introduce the non-dimensional phase speed

$$\psi = \bar{\omega}u_* \cos\theta/g ;$$

then $B = \bar{\omega}B^*$, where B^* is a universal function of ψ (Miles 1959). Inoue (1967, p. 32) adopts the form

$$B_0^* = (2\pi)^{-1}[.00139\ \exp\{-7000(\psi-.031)^2\}+.725\psi^2\exp(-.0004\psi^{-2})]. \tag{10}$$

Two forms of B^* have been implemented in subroutine CMPE26:

$$B_1^* = \max(0,\ \beta[\psi^2-.0004]), \tag{11}$$

where the choice $\beta = .1155$ yields the same asymptotic behavior as (9) for large ψ; &

$$B_2^* = \beta[(\psi^2-.0004)+(503.3+\{2042000+122040000\psi\}\{\psi-.031\}^2)^{-1}] \tag{12}$$

constructed as a rational approximation to (10). The form (12), with $\beta = .1066$, has been successfully used in duration-limited growth tests.

Pierson-Moskowitz spectrum. The total energy in a "fully developed" spectrum is

$$\tfrac{1}{4}\alpha g^2\omega_0^{-4} = \tfrac{1}{4}\alpha\beta^{-1}g^{-2}U^4, \tag{13}$$

where we adopt Pierson & Moskowitz' values $\alpha_0 = .0081$, $\beta = .74$. For immature spectra, Resio & Vincent (1977, p. 19) propose the law

$$\alpha = .037(Eg^2u_*^{-4})^{-.23}. \tag{14}$$

The exponent -.23 is a least-squares fit; Hasselmann et al. (1973, p. 37) found -.22; the parametric model of Hasselmann et al. (1976, p. 213) prescribes the exponent -.20. In order to preserve consistency with (13) we scale total energy by U^{-4}:

$$\alpha = \alpha_0 \varepsilon^{-.23} = \alpha_0 (4\alpha_0^{-1} \beta g^2 U^{-4} E)^{-.23}; \qquad (15)$$

with U in m sec^{-1} and E in m^2, $\alpha \propto .0007293789 E^{-.23} U^{.92}$.

Angular spreading. Mitsuyasu et al. (1975) obtain a credible fit to the spreading function proposed by Longuet-Higgins et al. (1963):

$$M(\omega,\theta) = G(s)(\tfrac{1}{2}+\tfrac{1}{2}\cos\theta)^s \qquad (16)$$

where s is a function of ω/ω_0 & G(s) is a normalizing factor such that

$$\int M(\omega,\theta)d\theta = 1.$$

Mitsuyasu finds that s has a maximum at $\omega_{peak} = .8^{\frac{1}{4}}\omega_0$, & that

$$s_{peak} = 11.5\ (\omega_{peak} u_{10}/g)^{-2.5}, \qquad (17)$$

where u_{10} is the wind speed at 10 meters. Thus, for the reference spectrum,

$$s_{peak} = 11.5[(\omega_{peak}/\omega_0)(\omega_0 u_*/g)(u_{10}/u_*)]^{-2.5};$$

so that a value of u_{10}/u_* is needed to compute s_{peak}. The range of u_{10} underlying (17) is 7 to 10 m/sec; we adopt

$$u_* = 0.34 \text{ m/sec}$$

as a representative value of u_* in that range. Then

$$u_{10} = 2.5 u_* \log(10/z_0),$$

where z_0 is computed from (7); and $u_{10}/u_* = 27.3484642$ (so that $u_{10} = 9.2985$ m/sec); whence $s_{peak} = 15.00496$.

For $\omega \neq \omega_{peak}$, Mitsuyasu finds

$$s/s_{peak} = \min[(\omega/\omega_{peak})^5, (\omega/\omega_{peak})^{-2.5}];$$

but our interpolation scheme for M gives difficulties for $s < 1$ and so we adopt the forms

$$s = \max[1,\ 15.00496\times\min[(\bar{\omega}/\omega_{peak})^{5},(\bar{\omega}/\omega_{peak})^{-2.5}]] \tag{18}$$

and

$$M(\bar{\omega},\theta) = \frac{(1+\cos\theta)^{s} - 1}{\int_{-\frac{1}{2}\pi}^{+\frac{1}{2}\pi}[(1+\cos\theta)^{s}-1]d\theta}\ . \tag{19}$$

It was found that separating the algorithm into growth, cut-back and angular redistribution produced oscillations in the angular spectrum at high frequencies: accordingly, these operations are interleaved inside an outer loop that cycles through frequency bands.

3.3.7.1 Wind field cycling

The table below, covering the 12 growth cycles of 6 time steps, sufficiently illustrates the interaction of a 1½-hour growth step with wind fields archived at 2-hour intervals.

ISTEP	WAX	t	t+Δt	t+½Δt	wind field read	t_{wind}
1	1	0.0	1.5	0.75	1	0.0
1	2	1.5	3.0	2.25	2	2.0
2	1	3.0	4.5	3.75	3	4.0
2	2	4.5	6.0	5.25	4	6.0
3	1	6.0	7.5	6.75	-	6.0
3	2	7.5	9.0	8.25	5	8.0
4	1	9.0	10.5	9.75	6	10.0
4	2	10.5	12.0	11.25	7	12.0
5	1	12.0	13.5	12.75	-	12.0
5	2	13.5	15.0	14.25	8	14.0
6	1	15.0	16.5	15.75	9	16.0
6	2	16.5	18.0	17.25	10	18.0

With the numbering here given, when prolonging a simulation,

LSKIP = INT(3*KSTEP1/2)-1

3.3.7.2 Sequence of Operations in growth and dissipation algorithm:

1. Read U and θ_w at grid point.
2. If U < 3.11 m/sec (≈ 6.045 knots) exit.
3. Compute u_* from U by solving the equations

   $u_* = .4U/\log_e(19.5/z_0)$,

   $z_0 = c_1/u_* + c_2 u_*^2 + c_3$,

   where $c_1 = .00001525 m^2 sec^{-1}$, $c_2 = .00001468 m^{-1} sec^2$,

   $c_3 = -.0000371 m$, and c_2 is chosen to agree with Garratt (1977, p. 922).
4. Compute κ_1 from u_* by (9).
5. Adjust θ_w for angle between true north and grid north. In the present SOWM these two directions are identical, and no adjustment is made.

6. Compute $\cos(\bar{\theta}-\theta_w)$ for midpoint $\bar{\theta}$ of each angular band used.

7. Compute $\omega_0 = .74^{\frac{1}{4}} g/U$ and $\omega_{peak} = .8^{\frac{1}{4}}\omega_0$.

8. Compute the total spectral energy E (all frequencies, all directions).

9. Compute the virtual reference spectrum $\alpha^{-1}T_0$ by (2), (17), (18), for all frequencies and all downwind directions. [N.B. No specific tables of upwind and downwind directions are kept; the sense of a direction is determined by examining the sign of $\cos(\bar{\theta}-\theta_w)$.]

10. The remaining steps (11-19) are enclosed in a loop that cycles through frequencies, beginning at the lowest.

11. Compute α by (15).

12. Compute the one dimensional spectral component

$$T(\bar{\omega}) = \sum T(\bar{\omega},\theta) \quad \text{(all directions)}.$$

13. If $T(\bar{\omega}) < \frac{1}{4}\alpha g^2(\omega_1^{-4}-\omega_2^{-4})$, cycle through directions to cut back: $T_{new}(\bar{\omega},\theta) = T(\bar{\omega},\theta)\times\frac{1}{4}\alpha g^2(\omega_1^{-4}-\omega_2^{-4})/T(\bar{\omega})$.

14. Dissipate opposing bands. Cycle through pairs of directions $\{\theta,\theta+\pi\}$: $\Delta = |T(\bar{\omega},\theta)-T(\bar{\omega},\theta+\pi)|/\{T(\bar{\omega},\theta)+T(\bar{\omega},\theta+\pi)\}$; $T_{new}(\bar{\omega},\theta) = \Delta\times T(\bar{\omega},\theta)$, $T_{new}(\bar{\omega},\theta+\pi) = \Delta\times T(\bar{\omega},\theta+\pi)$.

15. Compute the downwind energy

$$T_d = \sum_{|\theta-\theta_w|<\frac{1}{2}\pi} T(\bar{\omega},\theta) + \frac{1}{2}\sum_{|\theta,\theta_w|=\frac{1}{2}\pi} T(\bar{\omega},\theta).$$

If $T_d < \frac{1}{4}\alpha g^2\omega_0^{-4}[\exp(-\omega_0^4\omega_1^{-4})-\exp(-\omega_0^4\omega_2^{-4})]$ (underdeveloped band), go to step 16; otherwise to step 17. [In this model, at any time step, a frequency band undergoes growth or angular redistribution, but not both.]

16. Grow. Cycle through downwind directions: if

$T(\bar{\omega},\theta) \geq T_0(\bar{\omega},\theta)$, or $B^*(\bar{\omega},\theta) \leq 0$,

do nothing, otherwise

$$T_{new}(\bar{\omega},\theta) = MIN[T_0(\bar{\omega},\theta),\{T(\bar{\omega},\theta)e^{B\Delta t}+AB^{-1}(e^{B\Delta t}-1)\}].$$

Go to step 18.

17. Redistribute energy over angles. For each frequency band, cycle through downwind directions and compute

$$X(\bar{\omega},\theta) = MIN[T(\bar{\omega},\theta)-T_0(\bar{\omega},\theta),0],$$

$$Y(\bar{\omega},\theta) = MIN[T_0(\bar{\omega},\theta)-T(\bar{\omega},\theta),0].$$

Sum X and Y to obtain X_d and Y_d. Compute

$$\xi = X_d/T_d \text{ and } \eta = X_d^2/Y_dT_d.$$

Then

$$T_{new}(\bar{\omega},\theta) = T(\bar{\omega},\theta) - \xi X(\bar{\omega},\theta) + \eta Y(\bar{\omega},\theta).$$

18. Adjust the total energy E:

$$E_{new} = E_{old} - T_{old}(\bar{\omega}) + T_{new}(\bar{\omega}).$$

3.3.8 The spectral propagation algorithm

The physics of wave propagation in deep water is well understood as a result of the work of Barber & Ursell (1948), Groves & Melcer (1961) and Snodgrass et al. (1966). Each component in the two-dimensional spectrum travels along a great circle in its direction at the deep-water group velocity appropriate to its frequency. The development of an efficient and accurate computer algorithm to simulate this process has been particularly difficult.

Baer (1962) studied the simple first-order finite-difference analogue to the convective term (velocity-gradient technique) and concluded that it was inadequate if the quasi-discontinuous spatial distribution of wave energy was to be preserved. Such a scheme has nevertheless been used, for example by Barnett (1968). More recently Ewing (1971) has applied a fourth-order convective difference scheme, which he showed to be considerably more conservative than first-order schemes. A recent paper by Brian Golding (1979) indicates that the latest practice at the U.K. Meteorological Office, Bracknell, is to use a second-order Lax-Wendroff scheme with a polar stereographic grid.

The so-called jump technique was proposed by Baer (1962) to overcome the smoothing effects of the velocity-gradient technique. In the jump technique, wave energy is considered to be discontinuously distributed on the grid system; and spectral components are simply translated (jumped) to adjacent grid points after a sufficient number of time steps has elapsed to account for the quotient of the spacing of grid points by the propagation velocity. The FNWC operational Mediterranean spectral wave model described by Lazanoff, Stevenson & Cardone (1973) employs the jump technique. Uji & Isozaki (1972) have developed a more complicated version of the jump technique whereby lateral spreading and longitudinal dispersion associated with discrete directional spectral components are simulated.

The postulate central to the development of all schemes described above is the faithful propagation of monochromatic waves. However, waves on the ocean are not monochromatic; even a narrow-band swell has finite bandwidth. The error incident to a crude gradient scheme is of order $N^{\frac{1}{2}}$, where N is the number of time steps; the error inherent in neglecting bandwidth is of order N, and is the dominant error for long propagation distances. A conservation property considered essential has not been rigorously verified for schemes described above, and is susceptible of a priori calculation only on a flat earth: indeed, the numerical experiments of Uji & Isozaki (1972) did not extend beyond consideration of a flat earth. The property, which may be called integral conservation, states that, for any distribution of energy removed from land and from the edges of the map, the total energy integrated over all grid points shall be identically equal before and after a time step. The scheme submitted achieves integral conservation by the exclusive use of downstream interpolation.

After the propagation matrix has been calculated as sketched in §3.1.6, and read by the SOWM in the format stated in §3.1.5.7, the propagation proper reduces to KPART address calculations to check whether the transmitting point is land or sea, another KPART

address calculations to locate the transmitting spectral bins in the array SPOLD, and KPART multiplications and additions to compute the variance in the receiving spectral bin in SPNEW. See §3.3.6.3.3, step 12.

All propagation distances are less than 120 miles, guaranteeing stability for north-south propagation. The occasional jumps into triangles III and IV at high latitudes and low frequencies have not been extensively investigated for stability with this SOWM; but similar constructions in SOWMs for limited basins have caused no trouble. In a globe completely covered with water, the approximation adopted for convergence of meridians would lead to a slowly amplifying band of wash at the equator in directions 81°, 99°, 261°, 279°; in the model as submitted, the growth of this wash is blocked by sinks in Africa and South America.

3.4 Readback programs

3.4.1 DUMP13. Reads spectra from tape 13 in the format in which they were written by PRWAX2, and prints the spectra, with marginal totals, for a selected list (not more than 100) of grid points.
Input parameters (in calling sequence): KPOINT is the number of points to be dumped. KSTEP1, KSTEP2, KSTEP3 have the same meaning as in the subroutine WORK §3.3.6.2.1); they must have the same values they had in namelist $WHAT.
Input parameters (in namelist $WHERE): LPOINT is the list of points to be dumped. The points must be in ascending order; no check is made for land or for LLONG = 1, 2, 75, 76, but any point with those properties will produce a page of meaningless output.

3.4.1 DUMQ13. Reads spectra from tape 13 in the format in which they were written by QRWAX2 (§3.3.6.3.3), and prints the spectra, with marginal totals, for a selected list of grid points. Input parameters and usage are the same as for DUMP13. DUMQ13 does not use sub-

routine UNPAQQ (§3.3.6.4.2); only spectra at points to be printed are converted from integer to real. The mathematical method is the same as in UNPAQQ, viz reversing the steps, taken in PAQQ.

3.4.3 DUMP14. Reads significant height fields from DD14 in the format in which they were written by PRWAX2 or QRWAX2, and prints a table of coded latitude, coded longitude, and significant height.

4. APPLICATION OF MODELING STUDIES TO SEASAT DATA

4.1 Assimilation of Scatterometer Derived Surface Winds

It is a characteristic of all operational numerical weather prediction models and of most general circulation models, including the GMSF GCM, that planetary boundary layer (PBL) exchange processes are treated quite parametrically. That is fluxes of momentum, heat and moisture across the PBL are parameterized in terms of the wind, temperature and humidity at the lowest active level of the model which is usually near the top of the PBL, and surface temperature, roughness and moisture characteristics (boundary conditions). In most models, therefore, the near surface wind, which is the quantity sensed over the ocean by the SEASAT SASS, is not specified or forecast explicitly. (In the GMSF GCM, a surface wind is computed internally through a simple downward extrapolation of the wind from higher levels.) Initialization in such models is concerned primarily with the mass field and the windfield above the PBL.

The simulation studies described above avoided the problems of assimilation of surface wind data into models of the above type by synthesizing the simulated scatterometer winds at the lowest active level of the GMSF GCM, level 9, which is situated near the 950 mb level. The simulation study therefore implies perfect boundary layer physics, since no errors have been introduced in the simulation to account for the extrapolation of winds from the surface to level 9. Another simplification made in the simulation was the avoidance of the "aliasing problem", which derives from the fact that the SASS wind algorithm operates on colocated pairs of measured radar backscatter cross-section measurements to return up to four possible wind vector solutions at each cell on the sea surface sensed. While the wind speed differences between the wind vector solutions are typically very small, the wind directions differ significantly. In the four alias case, the directions may be nearly 90° apart. In the three alias case, two of the three vectors may be only 30° apart, while

the two alias solutions are usually 180° degrees apart.

Experiments with real SEASAT-A wind data will therefore require some modifications of the procedures used in the simulation study. As a part of this study, a preliminary and rather simple modification to the GMSF GCM was designed, coded and tested[1]. The modification was intended to satisfy two objectives: (1) provide a reasonable specification of the marine surface wind direction at each GCM grid point, each time step, to be used as a first guess in a SASS alias removal scheme (the modification as presently coded simply picks the SASS alias closest to the first guess); (2) allow the assimilated SASS surface wind speed and direction data to be extrapolated to the lowest prognostic level of the GCM.

The procedure devised to accomplish the objectives utilized a simplified version of the PBL model developed by Hoffert and Sud (1976). That model is used to diagnose the surface wind, defined as the effective neutral stability wind at the 19.5 meter height, from level 9 and surface information. The method accounts for baroclinicity in an approximate way by superimposing baroclinic turning of the wind in the PBL upon frictional turning in computing the surface wind direction.

The basic procedure for specification of the surface wind may be outlined as follows:

1. At each ocean GCM grid point assemble the following quantities: level 9 wind components u_9, v_9; level 8 wind components u_8, v_8; level 9 potential temperature θ_9, and humidity q_9; sea surface temperature, θ_s.
2. Compute a surface wind direction from level 9 and level 8 wind components using the vertical extrapolation scheme presently used in the GCM. The difference between the extrapolated surface wind direction and the level 9 wind is considered

---

[1] Oceanweather Inc. contributed primarily to the development of a functional description, and to evaluation of simple tests; coding was done by M. Helfand of GMSF.

the approximate baroclinic component, $\Delta\alpha_b$, of the turning of the wind in the PBL.

3. Compute the magnitude of the friction velocity, u_* from the simplified Hoffert-Sud parameterization; that is,

$$u_* = \sqrt{C_d} \times (u_9^2 + v_9^2)^{1/2}$$

where the PBL bulk drag coefficient C_d is computed as a function of the dimensional ratios h/z_0 and R_b, where h is boundary layer depth, z_0 is the roughness parameter and R_b is

$$R_b = \frac{gh(\theta_9 - \theta_s)}{\theta_s(u_9^2 + v_9^2)}$$

The calculation of C_d proceeds in two stages. First, the neutral drag coefficient C_{dn} is obtained by iteration between

$$C_{dn} = .15/(\log_e h/z_0)^2$$

and

$$z_0 = A/u_* + Bu_*^2 + C$$

where A, B, C are taken from Cardone (1969). The first guess of z_0 is taken as .0025 cm and h is taken to be the height of level 9. The drag coefficient C_{dn} then is modified to account for stability through functions, F_1, which are curve fits derived by Hoffert-Sud from their numerical PBL solutions:

$$C_d = C_{dn} \times F_1(R_b, h/z_0)$$

A separate set of curve fits, F_2, provide the frictional turning of the wind $\Delta\alpha_f$ between level 9 and the surface:

$$\Delta\alpha_f = F_2(R_b, h/z_0)$$

Given $\Delta\alpha_b$ and $\Delta\alpha_f$, the surface wind and stress direction are obtained directly. The effective

19.5 meter wind speed is defined simply by surface layer theory

$$|V_{19.5}| = 2.5u_* \log_e(1950/z_0)$$

The assimilation of SASS winds follows a slightly different procedure, as winds at the surface must be extrapolated upward to level 9. The assimilation proceeds in the following steps:

1. From the surface windfield computed as described above, interpolate surface wind directions to the locations of the SASS measurement cells, and where aliased solutions exist, choose the solution closest to the interpolated direction.
2. Since the SASS solution may be described equivalently in terms of $|V_{19.5}| = 2.5u_* \log_e(1950/z_0)$, or u_*, compute

$$R_b^* = \frac{gh(\theta_9 - \theta_s)}{\theta_s u_*^2}$$

and

$$z_0 = A/u_* + Bu_*^2 + C$$

3. Employ the simplified Hoffert-Sud model expressed in terms of F_3 and F_4 to compute the magnitude of the level 9 wind from

$$|V_9| = u_*^2/C_d$$

where

$$C_d = F_3(R_b^*, h/z_0)$$

4. Compute the frictional turning $\Delta\alpha_f$ from

$$\Delta\alpha_f = F_4(R_b^*, h/z_0)$$

5. Compute the level 9 wind direction from the surface direction, the computed frictional turning $\Delta\alpha_f$, and the baroclinic turning $\Delta\alpha_b$ of the guess field.

The modifications described above have been tested mainly to assume error free code. No SEASAT simulations were performed with the assimilation algorithm.

4.2 Impact of SEASAT-A data on large scale weather forecasting

The SEASAT-A data processing activity has progressed to the point where global SASS data sets will soon be produced, archived and disseminated. The study of weather patterns over the Northern Hemisphere by the SEASAT Simulations Studies Steering Group, (see Appendix A) has shown that the last month of the mission provides suitable conditions for the assessment of the impact on forecasts of data from SEASAT-A. An archive of all data necessary to perform the impact tests is being assembled at GMSF. The conventional analyses and data sources have already been assembled. The SEASAT-A data archive will consist initially of SASS data in terms of sensor data (backscatter coefficients) and geophysical data (wind vector aliases).

The first test of data impact, therefore, will be a straightforward application of the methodology of the simulation studies. Objective analyses of the conventional data sets will yield an estimate of Nature. Control analyses and forecasts will be produced exactly as in the simulation experiments. A SEASAT assimilation run will repeat the control assimilation and additionally include the asynoptic assimilation of data from SEASAT-A. As described above, the GCM model winds, interpolated to the mean cell location, will be extrapolated to the surface and used to remove the aliases. The satellite wind vectors will be extrapolated back to the lowest active level of the GCM and assimilated by the SCM as in the simulations. Forecasts from the SEASAT assimilation run will be compared with control forecasts, with objective analyses produced by the GMSF analysis package, and with an objective analysis produced by an analysis system independent of the GMSF GCM. If SMMR measurements are available they may be used to correct SASS data for attenuation by clouds and rain where possible; the SASS data will be rejected where such correction is requisite but not possible.

It may happen, contrary to expectation, that the first tests with real data from SEASAT will confirm the results of the simulation studies and show large beneficial impact on short-

range numerical weather forecasts. Rather, we expect the first tests to uncover problem areas requiring the development of more intricate experimental techniques. We anticipate at least one of the following scenarios, not to mention some combination of them: [1] the scatterometer data are not as accurate a measure of surface wind as expected; [2] the scatterometer is apparently a good measure of surface stress, but the parametrization of the planetary boundary layer in the GCM is too crude to utilize the data; [3] the use of the GCM forecast in the retrieval process results in the rejection of valid wind data from SEASAT-A; [4] the wind data are duly assimilated, but their effect on forecasts is not significant.

If an initial test should show large beneficial impact, the program of experiments can proceed to develop optimal assimilation methods incorporating, in addition to SEASAT, other remotely sensed data such as indirect soundings and winds from cloud trackings; and thence to design an operational satellite system. Problem [1] would require more sophisticated preprocessing techniques, based on geophysical reduction algorithms more complicated than those now before the SASS team. For example, backscatter may depend jointly on wind stress and large-scale surface roughness; to retrieve surface stress would require that a coupled GCM-SOWM be used in the assimilation. Problem [2] would place the emphasis on model development; as part of the simulation studies program, a hierarchy of modifications to the parameterization of the planetary boundary layer at GMSF has been formulated; while only the simplest modifications are being implemented, more complicated models can be made available as needed. Problem [3] would require more complicated assimilation procedures. One possibility is to increase the assimilation period to 3 or even 6 hours; so that several orbits of SEASAT-A can be processed jointly with ancillary satellite data (e.g. wind vectors from low-level cloud tracking), conventional ship and buoy reports, and model forecast information to provide an improved guess field for alias removal. A man-machine mix analogous to the "special

effort" procedures being implemented for the global weather experiment is a conceivable operation at this step, but obviously it should be implemented only if found to be necessary. Problem [4] would represent a confirmation of the earliest suspicions of the Simulation Studies Steering Committee, viz: that even accurate wind data should not significantly affect numerical forecasts because of the slight contribution of the surface layer to the overall energetics of synoptic-scale systems and because, in accordance with geostrophic adjustment theory, the model will reject the wind data dynamically. If so, surface winds from SEASAT would have to be combined with other data sets and, possibly external to the assimilation step, be extended to influence other variables, such as the pressure field. In any case, the joint assimilation of SEASAT winds and sounder information should be tried; a synergistic effect between the two kinds of data was apparent in an early simulation study.

4.3 Utilization of Wave Data from SEASAT-A in GSOWM.

There is already considerable evidence to support the validity of the wave heights to be retrieved from SEASAT-A. The concept of obtaining RMS wave height by analysing the shape of the return pulse to a radar altimeter has been proven; GEOS-3 has been routinely returning wave heights so retrieved for several years. The improved radar altimeter on SEASAT-A is likely to attain its objective of accuracy of ±0.5 m or ±10% in significant wave height. The wave height data are not now used operationally, though they are of potential benefit. Pierson & Salfi (1978) compared significant wave heights measured by GEOS-3 with operational northern hemisphere wave analyses produced at the U.S. Navy Fleet Numerical Weather Center (FNWC) for 44 orbit segments obtained during 1975 and 1976. The comparison revealed a significant bias in the wave analyses and occasional large differences over some orbit segments; the latter were attributed to poor specifications of windfield input to the wave model that generated the analyses. The wave heights from GEOS-3 were not compared with forecasts.

The basis of wave analysis and prediction at FNWC is a numerical

spectral wave specification model operated in a hindcast-forecast cycle twice daily, using windfield input data exclusively; in wave forecasting, unlike numerical weather prediction, initial wave conditions are not specified from wave data, which have always been too scarce to make such a specification profitable. GEOS-3 and now SEASAT-A, however, have altered the global wave measurement data base dramatically. As part of this study, a spectral wave specification model was adapted to the GMSF computer, to allow the development of methods for assimilating wave heights from SEASAT-A into a wave hindcast-forecast cycle based on that model.

Contemporary wave specification models have been reviewed recently by Cardone & Ross (1979). All such models are based upon the spectral energy balance equation, usually applied in its simplest form; that is, to surface gravity waves assumed to propagate through water of infinite depth that is otherwise at rest. In this form, the equation may be written

$$\frac{\partial}{\partial t} E(f,\theta,\vec{x},t) + \vec{C}_g(f,\theta)\times\Delta E(f,\theta,\vec{x},t) = S(f,\theta,\vec{x},t) \qquad (20)$$

where E is the energy density of the wave field described as a function of frequency f, direction of propagation θ, position $\vec{x}$, and time t; $\vec{C}_g$ is the deep-water group velocity vector; and S, the source function, represents all physical processes that transfer energy to or from the spectrum. Models of the so-called discrete type represent the spectrum E in terms of a number of spectral components (bands) of finite width, and successively simulate wave propagation (the homogenous part of (20)) and local energy transfers (the r.h.s. of (20)) in a series of discrete time steps on a grid overlaid on the basin of interest. Both rectangular and triangular grids have been used. In the model adapted to the GMSF, the spectrum is resolved into 192 components (16 directions × 12 frequencies), and the scheme reported by Greenwood & Cardone (1977) is used to propagate spectral components along archs of great circles and to refer the resulting propagation pattern to the GMSF GCM spherical grid. The source function S accounts

explicitly for energy transfers from the wind and implicitly for non-linear wave-wave interactions (Cardone et al. 1976). A discrete model is run operationally at FNWC to provide 72-hour forecasts for basins in the northern hemisphere, twice daily. Initial conditions $E(f,\theta,\vec{x},t_0)$ are calculated in a hindcast procedure using the same model and surface windfields produced by objective analysis of ship reports of wind and sea-level pressure.

An alternate model context for wave prediction, proposed recently by Hasselmann et al. (1976), is based on a parametric representation of the spectrum

$$E(f,\theta) = E(a_i,\ i=1,\ldots,n)$$

involving a relatively few parameters a_i. The JONSWAP spectrum, much used in this context, specifies the five parameters f_m, α, γ, σ_a, and σ_b; where f_m is the frequency of the spectral peak, α is the "equilibrium range" constant, γ is a peak enhancement factor, and σ_a and σ_b specify the width of the left and right sides of the spectral peak. The directional spread of energy is taken as symmetrical about the local wind direction. The parametric models are implemented by projecting the energy balance equation (20) including the source terms, onto a set of prognostic equations for the parameters of (21). Hasselmann et al. propose that for wind-generated seas only one or two parameters are necessary: their one-parameter model, for example, specifies a quasi-equilibrium relation between α and the non-dimensional peak frequency $\nu = f_m u_{10}/g$, where u_{10} is the wind speed 10 m above the sea surface. More complicated wave regimes require a hybrid model combining a parametric model of local sea with the propagation of swell in bands.

While discrete models have been fairly extensively applied, calibrated, and verified, there have been few studies comparing discrete spectral models with hybrid-parametric models. It appears, however, that some of the concepts advanced in the development of parametric models are suited to the development of techniques for assimilating remotely sensed wave data into a wave hindcast-forecast system. Significant wave height, the characteristic of

the sea surface measured by the radar altimeter on SEASAT-A, is an integral property of the spectrum and is therefore more appropriately assimilated in the parametric domain. It will therefore be necessary to incorporate some elements of parametric models into the GMSF SOWM for the purpose of assimilating significant wave height. The method will require, first, modification of the model so that at any desired grid point and time step the discrete spectral matrix can be partitioned into swell and wind sea; and the latter represented parametrically, in terms of total energy, peak frequency, and mean direction of wave travel. Then an algorithm may be developed that accepts updated values of total energy, wind speed, and wind direction, and adjusts the remaining parameters. In developing that algorithm by transforming the prognostic equations of Hasselmann et al., it appears that a more convenient pivotal quantity can be chosen than the non-dimensional peak frequency ν; Resio & Vincent (1977) show that the non-dimensional total energy ε, which in simple fetch-limited growth models is linearly related to the non-dimensional fetch, is a useful substitute for the latter in more complicated regimes.

The methods may be tested as follows. Given a run that assimilated real winds from SEASAT-A, use the surface winds specified therefrom at 3-hour intervals to drive the GMSF global SOWM until the hindcast wave field is independent of the initial conditions in the SOWM (usually several days). Then begin to assimilate significant wave heights from SEASAT-A. At grid points near the altimeter swath, partition the spectra into swell and parametric sea, deflate the measured significant height by the swell, and update the SOWM sea on the basis of the sea inferred from the measurement. Then, by integrating the updated parametric sea over the 192 frequency-direction bands, reconstruct the directional spectrum at the grid point and add the swell back in. A method of successive corrections in parameter space may be applied to blend the corrections into grid points adjacent to the subsatellite arcs treated at the assimilation step. The method assumes that the difference between modelled and measured wave height at a grid

point is primarily associated with the wind sea and therefore with local and recent errors in the windfield. This assumption is based on the intuitive notion that the continuous insertion of global wind and wave height data, if successful, would correct most errors in spectra in the zone of generation before they could be propagated any great distance. The assumption, however, needs to be tested.

5. SUMMARY AND CONCLUSIONS

Within the next year, high resolution global data sets consisting of measurements of marine surface wind, stress and significant wave height derived from SEASAT-A microwave sensors will be processed and made available for evaluation. Those data sets will be truly unique in providing global coverage of air-sea interfacial parameters that are at best poorly sensed from sparsely distributed ground based systems. Of great significance is the fact that the scale of motion sampled in the satellite resolution cell matches closely the synoptic scale and therefore is of great potential value in the initialization of large scale numerical weather forecasting and ocean sea state prediction models. Conventional anemometer measurements for example, do not adequately separate the turbulent and synoptic scale because of the short averaging interval characteristic of even the best surface based systems.

Preliminary evaluation of the performance of the SEASAT-A sensors of interest in this study (SASS,ALT,SMMR) suggests strongly that the design goals for measurement accuracy have been met. It remains to be demonstrated however, that skill in operational weather and sea state analyses and forecasts would increase if such data were available routinely from an operational SEASAT type satellite system.

The studies reported here provide a firm basis for the conduct of an experimental program to assess the potential of real SEASAT data. Three major accomplishments are reported. First, as part of a collaborative program with the GMSF, a series of observing system simulation experiments has been performed to assess the potential impact of marine surface wind data on numerical weather prediction. The experiments simulated the time continuous assimilation of remotely sensed surface wind data following a SEASAT-A orbit. When error-free winds were assimilated using a localized successive correction method, substantial impacts in simulated 72 hour forecasts of surface pressure were found over both land and ocean extratropical regions. The effect of nominal

SASS errors on the impacts were found to be small. The simulation studies suggest that marine surface wind data if accurate enough, can have a beneficial effect on numerical forecasts comparable to or even greater than the effect of accurate remotely sensed sounder data.

The second accomplishment was the development and implementation on the GMSF computer facility of a global spectral ocean surface wave specification model of contemporary formulation. The program models the generation, propagation and dissipation of surface gravity waves on a globe defined by the GMSF fine grid. Thus the model may be run in tandem with the GMSF GCM in either of three modes. In one mode, the model can be driven simply by analysis and forecast windfields specified by the GCM. In such a mode, the model serves to translate satellite induced impacts in surface windfield analyses and forecasts to surface wave analyses and forecasts. In another mode, the wave model itself might be used to assimilate remotely sensed significant wave height to reduce errors in initial wave spectra. Finally, should refined SASS geophysical retrieval algorithms require the knowledge of sea state for the optimum recovery of the surface wind and stress field, the GCM and GSOWM may be coupled to allow the retrieval and assimilation of surface winds of maximum attainable accuracy from scatterometer measurements.

Finally, this study included the design of algorithms for the assimilation of SASS surface data into the GMSF GCM and for the utilization of real SASS wind data and ALT wave height data into a coupled GCM-SOWM. The former algorithm has been implemented in an experimental version of the GMSF GCM to be used for the first real data tests. The latter algorithm is largely in the conceptual stage.

REFERENCES

Baer, L. 1962. An experiment in numerical forecasting of deep water ocean waves. Lockheed Missile and Space Company Report, LMSC-801296, San Diego, California

Barber, N. & F. Ursell. 1948. The generation and propagation of ocean waves and swell. Philos. Trans. Roy. Soc. London A 240: 257.

Barnett, T.P. 1968. On the generation, dissipation and prediction of ocean wind waves. J. Geophys. Res., 73, 513-529.

Blackmon, M.L., R.A. Madden, J.M. Wallace & D.S. Gutzler. 1979. Geographical variations in the vertical structure of geopotential height fluctuations. Submitted to Mon. Wea. Rev.

Born, G.H., J.A. Dunne & D.B. Lame. 1979a. Seasat mission overview. Science, 204, pp. 1405-1406.

Born, G.H., D.B. Lame & J.C. Wilkerson Eds. 1979b. GOASEX workshop report. Report 622-101, Jet Propulsion Laboratory, Pasadena, California (Internal document).

Cane, M., V.J. Cardone, I. Halberstam, M. Halem, & J. Ulrich. 1979. Observing system simulation and potential impact of marine surface wind data on numerical weather prediction. Submitted to Mon. Wea. Rev.

Cardone, V.J. 1969. Specification of the wind field distribution in the marine boundary layer for wave forecasting. Report TR-69-1, Geophy. Sci. Lab., New York University. Available from NTIS AD#702-490.

Cardone, V.J. 1977. Satellite observation systems and environmental forecasts: Progress and prospects. In Earth observation systems for resource management and environmental control, ed. Clough & Morley. New York: Plenum Publishing Corporation.

Cardone, V.J., W.J. Pierson, & E.G. Ward. 1976. Hindcasting the directional spectra of hurricane generated waves. J. of Petrol. Technology, 28, 385-394.

Cardone, V.J. & D.B. Ross. 1979. State-of-the-art wave prediction methods and data requirements. Ocean Wave Climate, Edited by M.D. Earle and A. Malahoff, Plenum Publishing Corporation, 1979, 61-91.

Ewing, J.A. 1971. A numerical wave prediction method for the North Atlantic Ocean. Deutsche Hydrographische Zeitschrift, 24, 241-261.

Garratt, J.R. 1977. Review of drag coefficients over oceans and continents. Mon. Wea. Rev. 105, 915-929.

Ghil, M., M. Halem, & R. Atlas. 1979. Time-continuous assimilation of remote-sounding data and its effect on weather forecasting. Mon. Wea. Rev., 107, 140-171.

Golding, B. 1979. Computer calculations of waves from wind fields. To be published in Proceedings of the IMA Conference on Power from Sea Waves. Ed. D.B. Court, Academic Press.

Greenwood, J.A. & V.J. Cardone. 1977. Development of a global ocean wave propagation algorithm. Final report to U.S. Navy Fleet Numerical Weather Central, Monterey, California, Contract N-00228-76-C-3081.

Groves, G.W. & J. Melcer. 1961. On the propagation of ocean waves on a sphere. Geofis. Ist. Mexico 1: 77.

Halem, M., V.J. Cardone, & R. Dilling. 1976. SEASAT impact on short term weather forecasting. In Meteorology Research Review, 1975. Institute for Space Studies, Goddard Space Flight Center, NASA.

Hasselmann, K., T.P. Barnett, E. Bouws, H. Carlson, D.E. Cartwright, K. Enke, J.A. Ewing, H. Gienapp, D.E. Hasselmann, P. Kruseman, A. Meerburg, P. Muller, D.J. Olbers, K. Richter, W. Sell & H. Walden. 1973. Measurements of wind-wave growth and swell decay during the Joint North Sea Wave Project (JONSWAP). Deutsche Hydrographische Zeitschrift, Supplement A8, 12.

Hasselmann, K., B. Ross, P. Müller, & W. Sell. 1976. A parametric wave prediction model. J. Phys. Oceanogr. 6, 200-228.

Hoffert, M. & Y. Sud. 1976. Similarity theory of the buoyantly interactive planetary boundary layer with entrainment. J. Atmos. Sci., 33, 2136-2151.

Inoue, T., 1967. On the growth of the spectrum of a wind generated sea according to a modified Miles-Phillips mechanism and its application to wave forecasting. Ph.D. dissertation, New York University.

Lazanoff, S.M., N. Stevenson & V.J. Cardone. 1973. A Mediterranean Sea wave spectral model. Tech. Note 73-1, Fleet Numerical Weather Central, Monterey, California.

Longuet-Higgins, M.S., D.E. Cartwright & N.D. Smith. 1963. Observations of the directional spectrum of sea waves using the motions of a floating buoy. In Ocean wave spectra: Proceedings of a conference sponsored by the U.S. Naval Oceanographic Office and the Division of Earth Scie ces, National Academy of Sciences/National Research Council: Easton, Maryland, May 1-4, 1961, 111-136. Englewood Cliffs, New Jersey, Prentice-Hall.

McCandless, S.W. & V.J. Cardone. 1976. SEASAT-A oceanographic systems and users. 27th International Astronautical Federation, Paper 76-061.

Miles, J.W. 1959. On the generation of surface waves by shear flows. Part II. J. Fluid. Mech. 6, 568-582.

Mitsuyasu, H., F. Tasai, T. Suhara, S. Mizuno, M. Okhusu, T. Honda, & K. Rikiishi. 1975. Observations of the directional spectrum of ocean waves using a cloverleaf buoy. Journal of Physical Oceanography 5, 750-760.

Pierson, W.J., & R.E. Salfi. 1978. Verification results for the Spectral Ocean Wave Model (SOWM) by means of significant wave height measurements made by the GEOS-3 spacecraft. NASA Contractor's Report NCR-62089. NASA Wallops Flight Center.

Priestley, J.T. 1965. Correlation studies of pressure fluctuations on the ground beneath a turbulent boundary layer. M.S. thesis. University of Maryland.

Resio, D.T., & C.L. Vincent. 1977. A numerical hindcast model for wave spectra on water bodies with irregular shoreline geometry I. Test of nondimensional growth rates. Miscellaneous paper H-77-9, Hydraulics Laboratory, U.S. Army Engineer Waterways Experiment Station, Vicksburg, Mississippi.

Snodgrass, F.E., et al. 1966. Propagation of ocean swell across the Pacific. Philos. Trans. Roy. Soc. London A 259: 431.

Snyder, R.L. & C.S. Cox. 1966. A field study of the wind generation of ocean waves. Journal of Marine Research 24, 141-178.

Uji, T. & I. Isozaki. 1972. The calculation of wave propagation in the numerical prediction of ocean waves. Papers in Meteorology and Geophysics, Tokyo, 23, 347-359.

Appendix A: Papers, presentations, meeting participation supported under this contract.

Papers

1. Realistic simulations of the global observing system and of SEASAT-A marine wind data. M. Cane, V.J. Cardone, I. Halberstam, M. Halem, J. Ulrich. Submitted to Mon. Wea. Rev.

2. Observing system simulation and potential impact of marine surface wind data on numerical weather prediction. Same authors as above. This paper is a substantial revision of the above paper with considerable material added. Submitted to Mon. Wea. Rev. in April 1979 as a revision of 1.

Presentations

1. Realistic simulations of the global observation system and of SEASAT-A marine wind data. M. Cane and V. Cardone. Presented by M. Cane at the 1978 Fall Meeting of the American Geophysical Union, San Francisco, Calif. (Abstract attached).

2. Results of SEASAT simulation studies. V. Cardone. Informal presentation to the interagency NOSS Advisory Panel, July, 1978, Jet Propulsion Laboratory, Pasadena, Calif.

3. The contribution of SEASAT satellite capabilities to marine forecasting. V. Cardone. Presented to International Maritime Weather Conference and Exhibit, February 7, 1979, New York.

4. Results of GLAS SEASAT Simulation Studies. V. Cardone. Presented to S^{4}G SEASAT Planning Meeting, June 6,7, 1979 Atmospheric Environmental Service, Downsview, Ontario

Meetings

1. SASS Team Meeting, Langley Research Center, August 15-16, 1978
2. S^4G SEASAT Planning Meeting, June 6-7, 1979, AES Downsview, Ontario
3. Travel to GMSF, Greenbelt, Md. by Oceanweather staff.
   1978: April 13-14, May 24-25, June 26-27, August 2, August 28, September 26-27, November 14-15, December 20-21.
   1979: April 5-6, April 24-25, July 5-6, August 28.

REALISTIC SIMULATIONS OF THE GLOBAL OBSERVING SYSTEM AND OF SEASAT-A MARINE WIND DATA

Mark A. Cane (NASA/Goddard Space Flight Center, Greenbelt, Md. 20771)
Vincent J. Cardone (Oceanweather Inc., White Plains, N.Y. 10601)

A 30-day history run made with the Goddard Modelling and Simulation Facility General Circulation Model (GCM) was used to fabricate simulated observations at the times and locations of the conventional surface, radiosonde and ship reports actually received during Feb. 1976. The fabricated observations, suitably degraded for instrument and sampling errors, were then used to create analysed fields on the GCM grid in an analysis-forecast cycle like those in use at major meteorological centers. The control fields so produced are much more representative of actual analyses than those produced by perturbation of initial states with random errors. Significantly, the forecast error growth in 5 simulated 72-hour forecasts from the control states is similar to that found in operational numerical forecasts. Further experiments simulated the addition of surface winds derived from SEASAT-A to the control run. These winds were fabricated directly for the GCM grid points intercepted by a SEASAT-A scatterometer swath, and were assumed to be error-free and representative of the lowest active level of the GCM. Two different asynoptic assimilation methods were used: direct insertion (DIM) and successive correction (SCM). Assimilation of winds by DIM was found to produce slight improvements in simulated analyses and forecasts. The SCM experiments, however, resulted in 40% reductions of error in the specification and 72-hour forecast of sea-level pressure and low- and mid-tropospheric winds. Preliminary results will be presented from experiments in progress, which include the simulation of errors expected in scatterometer-derived winds; and, as available, from experiments using real SEASAT-A global wind data sets.

1. 022075 CARDONE
2. 1978 Fall Meeting
3. Oceanography/Meteorology
4. Seasat
5. No
6. No
7. 0%
8. As in item 1
9. Not required

APPENDIX B

GSOWM Computer Program Listing

PROGRAM PRELIMS/MAIN

```
      COMMON
     $/YPARAM/ LLAT,LLONG,LPNT1,LPNT2,FREQ(14),FREQ1,FREQ2,SPACE(2)
     $   ,WEDGE,DIREC(20),DELT
     $/YSHORT/ TLAT(3,73),TLONG(2,76)
     $/YYOLTB/ JTABLE,TABLE(4,20,73)
     $/YYTRIG/ DLAT,COSS,DANGLE,CLAT,TRAVEL,          RAD,CTR,STR,
     $   OMIN,017,RAT(3,73)
      INTEGER*2 JTABLE(16,20,73)
      REAL*8 DLAT(73),COSS(20),DANGLE(20),CLAT(2,73),TRAVEL(14),
     $   CTR(14),STR(14),RAD,OMIN,017
      DATA L13,L14/13,14/
      FREQ1 = .04
      FREQ2 = .20
      WEDGE = 9.
      DELT = 3.
      CALL GGRID (L13)
C     ENDFILE L13
      CALL BANDS
      CALL TRIG
      DO 10 IA = 1,14
        CALL OUTBND (IA)
        CALL INBND (L14+IA)
10    CONTINUE
      CALL TRANSP (L14,L13)
      ENDFILE L13
      STOP
      END
```

```
      SUBROUTINE GGRID (LU)
      COMMON
     $/YPARAM/ LLAT,LLONG,LPNT1,LPNT2,FREQ(14),FREQ1,FREQ2,SPACE(2)
     $   ,WEDGE,DIREC(20),DELT
     $/YSHORT/ TLAT(3,73),TLONG(2,76)
     $// JLAT,JLONG,ALAT(76,73),ALONG(76,73)
      NAMELIST
     $/LIST02/ LLAT,LLONG,LPNT1,LPNT2,SPACE
      INTEGER*2 JLAT(76,73),JLONG(76,73)
      DATA LOUT/6/
      REWIND LU
      LLAT = 73
      LLONG = 76
      LPNT1 = LLAT*(LLONG-4)
      LPNT2 = LLAT*LLONG
      SPACE(1) = .999848
      SPACE(2) = .325568
      DO 27 IA = 1,2
        SPACE(IA) = SQRT(120.**2+(150.*SPACE(IA))**2)
27    CONTINUE
      WRITE (LOUT,LIST02)
      DO 32 IA = 1,73
        TLAT(1,IA) = 2*IA-74
        TLAT(2,IA) = 300.*COS(.0174533*TLAT(1,IA))
        TLAT(3,IA) = SQRT(144E2+.25*TLAT(2,IA)**2)
32    CONTINUE
      WRITE (LOUT,34) (I,(TLAT(J,I),J=1,3),I=1,73)
34    FORMAT (/(5(I5,F5.0,2F7.2)))
      DO 39 IA = 1,76
        TLONG(2,IA) = 5*IA-100
        IF (TLONG(2,IA).GE. 180.) TLONG(2,IA) = TLONG(2,IA)-360.
        TLONG(1,IA) = TLONG(2,IA)+2.5
39    CONTINUE
      WRITE (LOUT,41) (I,TLONG(1,I),TLONG(2,I),I=1,76)
41    FORMAT (/(6(I5,2F7.1)))
      DO 50 LAT = 1,73
        MLAT = 2-MOD(LAT,2)
        DO 49 LONG = 1,76
          JLAT(LONG,LAT) = LAT
          JLONG(LONG,LAT) = LONG
          ALAT(LONG,LAT) = TLAT(1,LAT)
          ALONG(LONG,LAT) = TLONG(MLAT,LONG)
49      CONTINUE
50    CONTINUE
      WRITE (LOUT,52) (I,JLAT(I,1),JLONG(I,1),ALAT(I,1),ALONG(I,1)
     $   ,I=1,5548)
52    FORMAT (/(5(I7,2I3,F6.1,F7.1)))
C     WRITE (LU) ALAT
C     WRITE (LU) ALONG
      RETURN
      END
```

```
      SUBROUTINE BANDS
      COMMON
     $/YPARAM/ LLAT,LLONG,LPNT1,LPNT2,FREQ(14),FREQ1,FREQ2,SPACE(2)
     $   ,WEDGE,DIREC(20),DELT
      DATA LOUT/6/
      NAMELIST
     $/LIST03/ DIREC,FREQ,DELT
      DO 61 IA = 1,20
        DIREC(IA) = 18*IA-5
61    CONTINUE
      RAT = 5.**.08
      FREQ(1) = FREQ1
      DO 66 IA = 1,13
        FREQ(IA+1) = RAT*FREQ(IA)
66    CONTINUE
      WRITE (LOUT,LIST03)
      RETURN
      END
```

```
      SUBROUTINE TRIG
      COMMON
     $/YPARAM/ LLAT,LLONG,LPNT1,LPNT2,FREQ(14),FREQ1,FREQ2,SPACE(2)
     $   ,WEDGE,DIREC(20),DELT
     $/YSHORT/ TLAT(3,73),TLONG(2,76)
     $/YYTRIG/ DLAT,COSS,DANGLE,CLAT,TRAVEL,          RAD,CTR,STR,
     $  OMIN,O17,RAT(3,73)
      REAL*8 DLAT(73),COSS(20),DANGLE(20),CLAT(2,73),TRAVEL(14),
     $  CTR(14),STR(14),RAD,OMIN,O17
      DATA LOUT/6/
      REAL*8 PI4,SPEED
      PI4 = DATAN(1D0)
      O17 = PI4/45D0
      OMIN = PI4/27D2
      RAD = 45D0/PI4
      SPEED = 9.806D0/16D0/PI4*36D2/1852D0
C COMPUTE TRAVEL (NAUTICAL MILES PER TIME STEP)
      DO 78 IA = 1,14
        TRAVEL(IA) = SPEED*DELT/FREQ(IA)
        CTR(IA) = DCOS(TRAVEL(IA)*OMIN)
        STR(IA) = DSIN(TRAVEL(IA)*OMIN)
78    CONTINUE
      WRITE (LOUT,80) TRAVEL
80    FORMAT ('0TRAVEL'/(7D18.11))
C COMPUTE AREA RATIO
      DO 85 IA = 1,72
        RAT(1,IA+1) = TLAT(2,IA+1)/TLAT(2,IA)
        RAT(2,IA) = 1.
        RAT(3,IA) = TLAT(2,IA)/TLAT(2,IA+1)
85    CONTINUE
      RAT(1,1) = 0.
      RAT(2,73) = 1.
      RAT(3,73) = 0.
C COMPUTE TABLE OF DIRECTIONS
      DO 94 IA = 1,20
        DANGLE(IA) = DIREC(IA)
        IF (DIREC(IA).GT. 180.) DANGLE(IA) = DANGLE(IA)-36D1
        DANGLE(IA) = DANGLE(IA)*O17
        COSS(IA) = DCOS(DANGLE(IA))
94    CONTINUE
C COMPUTE TABLE OF DOUBLE PRECISION COLATITUDES
      DO 99 IA = 1,73
        DLAT(IA) = (90.-TLAT(1,IA))*O17
        CLAT(1,IA) = DCOS(DLAT(IA))
        CLAT(2,IA) = DSIN(DLAT(IA))
99    CONTINUE
      RETURN
      END
```

```
      SUBROUTINE OUTBND (I)
      COMMON
     $/YPARAM/ LLAT,LLONG,LPNT1,LPNT2,FREQ(14),FREQ1,FREQ2,SPACE(2)
     $   ,WEDGE,DIREC(20),DELT
     $/YSHORT/ TLAT(3,73),TLONG(2,76)
     $/YYOUTB/ JTABLE,TABLE(4,20,73)
     $/YYTRIG/ DLAT,COSS,DANGLE,CLAT,TRAVEL,          RAD,CTR,STR,
     $   OMIN,DTR,RAT(3,73)
      INTEGER*2 JTABLE(16,20,73)
      REAL*8 DLAT(73),COSS(20),DANGLE(20),CLAT(2,73),TRAVEL(14),
     $   CTR(14),STR(14),RAD,OMIN,DTR
      REAL*8 SS,SM(4),DLAT2,DAZ,DTR,DLONG
      INTEGER*2 VERTEX(9,4,8)
      DATA LOUT/6/
      DATA VERTEX/
     $   1,1,0,0,1,0,-76,-75,0,0,1,0,-1,0,0,-1,-76,0,1,0,1,2*-1,
     $   0,-77,-1,-76,0,1,0,-2,2*-1,-2,-77,-1,
     $   1,1,0,1,0,0,-75,-76,0,0,1,0,1,1,0,1,-75,0,1,0,1,2,1,1,
     $  -74,1,-75,0,1,0,2,2,1,2,-74,1,
     $   2*-1,0,0,1,0,76,77,0,0,-1,0,-1,0,0,-1,76,0,-1,0,3*-1,0,
     $   75,-1,76,0,-1,0,-2,2*-1,-2,75,-1,
     $   2*-1,0,1,0,0,77,76,0,0,-1,0,1,0,0,1,77,0,-1,0,-1,2,1,1,
     $   78,1,77,0,-1,0,2,2,1,2,78,1,
     $   1,1,0,-1,0,0,-77,-76,0,0,1,0,2*-1,0,-1,-77,0,1,0,1,-2,
     $   2*-1,-78,-1,-77,0,1,0,2*-2,-1,-2,-78,-1,
     $   1,1,0,0,-1,0,-76,-77,0,0,1,0,1,0,0,1,-76,0,1,0,3*1,0,
     $  -75,1,-76,0,1,0,2,1,1,2,-75,1,
     $   2*-1,0,-1,0,0,75,76,0,0,-1,0,2*-1,0,-1,75,0,-1,0,-1,-2,
     $   2*-1,74,-1,75,0,-1,0,2*-2,-1,-2,74,-1,
     $   2*-1,0,0,-1,0,76,75,0,0,-1,0,1,0,0,1,76,0,-1,0,-1,1,1,0,
     $   77,1,76,0,-1,0,2,1,1,2,77,1/
      KFREQ = I
      DTR = TRAVEL(KFREQ)*OMIN
      RADIUS = TRAVEL(KFREQ)
      WRITE (LOUT,107) KFREQ,FREQ(KFREQ),RADIUS
107   FORMAT (1H1,I2,F10.7,F10.4)
      DO 110 IA = 1,5840
        TABLE(IA,1,1) = 0.
110   CONTINUE
      DO 113 IA = 1,23360
        JTABLE(IA,1,1) = 0.
113   CONTINUE
      DO 205 LAT = 1,73
        KWAD1 = 4*MOD(LAT,2)
        WRITE (LOUT,116) LAT,TLAT(1,LAT)
116     FORMAT ('0LAT =',I3,'  LATITUDE =',F6.1/)
        DO 202 IDIREC = 1,20
          KWAD2 = KWAD1+IDIREC/11
C SOLVE SPHERICAL TRIANGLE
          DLAT2 =DARCOS(CTR(KFREQ)*CLAT(1,LAT)+
     $       STR(KFREQ)*CLAT(2,LAT)*COSS(IDIREC))
          SS = .5D0*(DLAT(LAT)+DTR+DLAT2)
          SM(1) = DSIN(SS)
          SM(2) = DSIN(SS-DLAT(LAT))
          SM(3) = DSIN(SS-DTR)
          SM(4) = DSIN(SS-DLAT2)
          DLONG = 2D0*DATAN(DSQRT(SM(2)*SM(4)/(SM(1)*SM(3))))
          DAZ = 2D0*DATAN(DSQRT(SM(3)*SM(4)/(SM(1)*SM(2))))
C INTERPOLATING FACTORS FOR LATITUDE
          FLAT = DLAT2-DLAT(LAT)
          IF (FLAT .GT. 0.) KWAD2 = KWAD2+2
          FLAT = ABS(FLAT)*28.64789
          IF (FLAT .GT. 1.) STOP 130
C INTERPOLATING FACTORS FOR LONGITUDE
          FLONG = DLONG
```

```
            IF (FLONG .GT. 4.) STOP 133
            F1 = .5*(FLONG-FLAT)
            F2 = .5*(FLONG+FLAT)
C INTERPOLATING FACTORS FOR AZIMUTH
            FAZ = DAZ
            IF (IDIREC .GT. 10) FAZ = -FAZ
            FAZ = 180.-57.29578*FAZ
            FAZ = FAZ/18.
            KAZ = FAZ
            GAZ = FAZ-FLOAT(KAZ)-.5
            IF (GAZ .LT. 0.) GO TO 149
            FAZ1 = 1.-GAZ
            FAZ2 = GAZ
            KAZ1 = 1+KAZ
            KAZ2 = 2+KAZ
            IF (KAZ2 .EQ. 21) KAZ2 = 1
            GO TO 155
149         CONTINUE
            FAZ1 = 1.+GAZ
            FAZ2 = -GAZ
            KAZ1 = 1+KAZ
            KAZ2 = KAZ
            IF (KAZ2 .EQ. 0) KAZ2 = 20
155         CONTINUE
            IF (F1 .LT. 0.) GO TO 160
            IF (F1 .GT. 1.) GO TO 175
            IF (F2 .LT. 1.) GO TO 165
            GO TO 170
C TRIANGLE I
160         ITR = 1
            TABLE(1,IDIREC,LAT) = F2
            TABLE(2,IDIREC,LAT) = -F1
            TABLE(3,IDIREC,LAT) = 1.-FLAT
            GO TO 179
C TRIANGLE II
165         ITR = 2
            TABLE(1,IDIREC,LAT) = F1
            TABLE(2,IDIREC,LAT) = FLAT
            TABLE(3,IDIREC,LAT) = 1.-F2
            GO TO 179
C TRIANGLE III
170         ITR = 3
            TABLE(1,IDIREC,LAT) = F2-1.
            TABLE(2,IDIREC,LAT) = 1.-FLAT
            TABLE(3,IDIREC,LAT) = 1.-F1
            GO TO 179
C TRIANGLE IV
175         ITR = 4
            TABLE(1,IDIREC,LAT) = F1-1.
            TABLE(2,IDIREC,LAT) = FLAT
            TABLE(3,IDIREC,LAT) = 2.-F2
179         DO 183 IA = 1,3
              JTABLE(4*IA-3,IDIREC,LAT) =
     $          VERTEX(IA,ITR,KWAD2+1)+LAT
              JTABLE(4*IA-2,IDIREC,LAT) = VERTEX(IA+6,ITR,KWAD2+1)
              JTABLE(4*IA,IDIREC,LAT) = VERTEX(IA+3,ITR,KWAD2+1)
              JTABLE(4*IA-1,IDIREC,LAT) = KAZ1
183         CONTINUE
C TURN FRACTION OF ENERGY INTO BAND KAZ2
            DO 194 IA = 1,3
              GAZ = TABLE(IA,IDIREC,LAT)-FAZ2
              IF (GAZ .LT. 0.) GO TO 192
              TABLE(IA,IDIREC,LAT) = GAZ
              TABLE(4,IDIREC,LAT) = FAZ2
             JTABLE(13,IDIREC,LAT) = JTABLE(4*IA-3,IDIREC,LAT)
              JTABLE(14,IDIREC,LAT) = JTABLE(4*IA-2,IDIREC,LAT)
              JTABLE(16,IDIREC,LAT) = JTABLE(4*IA,IDIREC,LAT)
              JTABLE(15,IDIREC,LAT) = KAZ2
              GO TO 195
192           JTABLE(4*IA-1,IDIREC,LAT) = KAZ2
              FAZ2 = -GAZ
194         CONTINUE
```

```
C ADJUST ENERGY FOR CONVERGENCE OF MERIDIANS
            DO 200 IA = 1,4
              KA = JTABLE(4*IA-3,IDIREC,LAT)-LAT
              IF (KA .NE. 0) TABLE(IA,IDIREC,LAT) =
     $          TABLE(IA,IDIREC,LAT)*RAT(KA+2,LAT)
200         CONTINUE
202       CONTINUE
          IF(LAT.EQ.73)  WRITE (LOUT,204) ((JTABLE(4*I-3,J,LAT),
     $      JTABLE(4*I-2,J,LAT),JTABLE(4*I-1,J,LAT),
     $      JTABLE(4*I,J,LAT),TABLE(I,J,LAT),I=1,4),J=1,20)
204       FORMAT (4(I5,I4,2I3,F9.6))
205     CONTINUE
        RETURN
        END
```

```
      SUBROUTINE INBND (IN)
      COMMON
     $/YOUTB/ JTABLE,TABLE(4,20,73)
     $//              TAB2(6,20,73),MOOD,JTAB2
      INTEGER*2 JTABLE(16,20,73),JTAB2(13,20,73),MOOD(3,25)
      DATA LOUT/6/
      LU = IN
      REWIND LU
      DO 235 IA = 1,25
        MOOD(1,IA) = -21280
        MOOD(2,IA) = 0
        MOOD(3,IA) = +21280
235   CONTINUE
      DO 238 IA = 1,8760
        TAB2(IA,1,1) = 0.
238   CONTINUE
      DO 241 IA = 1,18980
        JTAB2(IA,1,1) = 0
241   CONTINUE
      DO 256 LAT = 1,73
        DO 255 IDIREC = 1,20
          DO 254 IA = 1,4
            KLAT = JTABLE(4*IA-3,IDIREC,LAT)
            IF (KLAT .EQ. 0) GO TO 254
            IF (KLAT .EQ. 74) GO TO 254
            KDIREC = JTABLE(4*IA-1,IDIREC,LAT)
            KOUNT = JTAB2(1,KDIREC,KLAT)+1
            IF (KOUNT .EQ. 7) STOP 250
            JTAB2(2*KOUNT,KDIREC,KLAT) =
     $        JTABLE(4*IA-2,IDIREC,LAT)
            JTAB2(2*KOUNT+1,KDIREC,KLAT) =
     $        MOOD(LAT,1)+280*JTABLE(4*IA,IDIREC,LAT)+
     $        14*(IDIREC-KDIREC)
            TAB2(KOUNT,KDIREC,KLAT) = TABLE(IA,IDIREC,LAT)
            JTAB2(1,KDIREC,KLAT) = KOUNT
254       CONTINUE
255     CONTINUE
256   CONTINUE
      DO 263 LAT = 1,73
        WRITE (LU)
     $    (JTAB2(I,1,LAT),I=1,260),(TAB2(I,1,LAT),I=1,120)
        IF(LAT.NE.73) GO TO 263
        DO 262 IDIREC = 1,20
          KOUNT = JTAB2(1,IDIREC,LAT)
          WRITE (LOUT,264) KOUNT,
     $      (JTAB2(2*I,IDIREC,LAT),JTAB2(2*I+1,IDIREC,LAT),
     $      TAB2(I,IDIREC,LAT),I=1,KOUNT)
262     CONTINUE
263   CONTINUE
264   FORMAT (I2,6(I5,I7,F9.6))
      REWIND LU
      RETURN
      END
```

```
      SUBROUTINE TRANSP(IOLD,NEW)
      COMMON/YSHORT/TLAT(3,73),TLONG(2,76)
     $//JTAB3(13,20),TAB3(6,20),JTAB4(13,14,20,73),TAB4(6,14,20,73)
      INTEGER*2 JTAB3,JTAB4
      DATA LOUT/6/
  264 FORMAT(I2,6(I5,I7,F9.6))
      LU=IOLD
      LU2=NEW
      DO 293 LAT=1,73
      DO 285 IFREQ=1,14
      LU1=LU+IFREQ
      READ(LU1) JTAB3,TAB3
      DO 284 IDIREC=1,20
      DO 278 IA=1,13
      JTAB4(IA,IFREQ,IDIREC,LAT)=JTAB3(IA,IDIREC)
  278 CONTINUE
      DO 283 IA=1,6
      TAB4(IA,IFREQ,IDIREC,LAT)=TAB3(IA,IDIREC)
  283 CONTINUE
  284 CONTINUE
  285 CONTINUE
      WRITE(LOUT,294) LAT,TLAT(1,LAT)
      DO 292 IA=1,280
      KOUNT=JTAB4(1,IA,1,LAT)
C     WRITE(LOUT,264)
C    $KOUNT,(JTAB4(2*I,IA,1,LAT),JTAB4(2*I+1,IA,1,LAT),
C    $TAB4(I,IA,1,LAT),I=1,KOUNT)
  292 CONTINUE
  293 CONTINUE
  294 FORMAT(' TRANSPOSED PROPAGATE TABLE, LAT=',I3,'  LATITUDE =',
     $  F6.1/)
      WRITE(LU2) JTAB4
      WRITE(LU2) TAB4
      STOP 303
      END
```

PROGRAM ICEDECK

```
      INTEGER*2 LANSEA(76,73),LAND1(76,35),LAND2(76,20),LAND3(76,18)
      EQUIVALENCE
     $   (LAND1(1,1),LANSEA(1,1)),(LAND2(1,1),LANSEA(1,36)),
     $   (LAND3(1,1),LANSEA(1,56))
      DATA LLAND,LOUT/11,6/
10    FORMAT(2X,212,2X,72I1,2X,2I1)
      DATA LAND1/4*2,3*1,10*2,36*1,23*2,23*2,27*1,26*2,
     $   25*2,23*1,28*2,39*2,1,1,2,1,33*2,380*2,5*2,1,70*2,
     $   4*2,1,71*2,4*2,1,1,70*2,4*2,1,1,70*2,4*2,1,1,47*2,1,22*2,
     $   4*2,1,1,70*2,5*2,1,1,69*2,4*2,3*1,69*2,5*2,3*1,46*2,1,21*2,
     $   4*2,4*1,39*2,1,1,27*2,5*2,4*1,39*2,3*1,25*2,
     $5*2,4*1,14*2,1,1,17*2,3*1,2,4*1,26*2,
     $   5*2,5*1,13*2,3*1,16*2,8*1,26*2,
     $   5*2,4*1,13*2,4*1,16*2,8*1,26*2,
     $   5*2,5*1,12*2,4*1,16*2,8*1,26*2,
     $   5*2,5*1,12*2,4*1,16*2,7*1,27*2,
     $   5*2,6*1,13*2,3*1,15*2,7*1,27*2,
     $   5*2,6*1,12*2,3*1,17*2,6*1,27*2,
     $   5*2,7*1,10*2,5*1,17*2,5*1,27*2,
     $   4*2,7*1,10*2,6*1,17*2,1,1,2,1,28*2,
     $   4*2,8*1,10*2,6*1,17*2,1,1,29*2,
     $   4*2,7*1,10*2,6*1,18*2,1,2,1,28*2,
     $   4*2,8*1,10*2,5*1,16*2,1,32*2,
     $   3*2,9*1,10*2,5*1,14*2,1,5*2,1,1,27*2,1,
     $   3*2,9*1,10*2,5*1,20*2,4*1,24*2,1,
     $   3*2,8*1,10*2,6*1,12*2,1,3*2,1,2,2,1,1,26*2,1/
      DATA LAND2/3*2,8*1,10*2,7*1,14*2,1,1,2,1,29*2,1,
     $   3*2,6*1,12*2,7*1,11*2,1,2,1,1,2,1,30*2,1,
     $   4*2,5*1,12*2,8*1,10*2,1,2,2,1,33*2,
     $   3*2,6*1,12*2,8*1,9*2,1,1,2,2,1,32*2,1,
     $   4*2,5*1,8*2,12*1,15*2,1,31*2,
     $   3*2,4*1,9*2,13*1,14*2,1,31*2,1,
     $   2,2,1,2,3*1,10*2,13*1,10*2,1,3*2,1,29*2,1,2,
     $   1,1,14*2,12*1,6*2,1,5*2,1,33*2,1,1,
     $   2,1,1,13*2,13*1,5*2,1,1,3*2,1,1,32*2,1,1,2,
     $   1,15*2,13*1,5*2,1,4*2,1,1,30*2,1,1,3*2,
     $   1,1,14*2,15*1,3*2,1,1,2,2,3*1,30*2,3*1,2,2,
     $   2,1,2,1,12*2,10*1,2,4*1,3*2,1,1,2,2,1,1,30*2,1,1,2,1,2,1,
     $   3*2,1,12*2,15*1,2,2,9*1,29*2,1,3*2,1,
     $   3*2,1,12*2,10*1,2,3*1,2,2,11*1,27*2,1,4*2,1,
     $   17*2,9*1,2,3*1,2,12*1,27*2,1,1,4*2,
     $   2,2,1,13*2,27*1,28*2,1,2,2,1,2,
     $   3*1,15*2,11*1,2,14*1,24*2,7*1,2,
     $   3*1,14*2,7*1,2,2,17*1,25*2,7*1,2,
     $   4*1,14*2,4*1,5*2,17*1,2,2,1,21*2,8*1,
     $   4*1,15*2,1,1,5*2,3*1,2,13*1,2,1,2,1,20*2,9*1/
      DATA LAND3/
     $   4*1,14*2,1,3*2,1,2,2,1,1,2,1,2,13*1,2,1,2,2,1,19*2,9*1,
     $   4*1,13*2,1,1,4*2,22*1,21*2,10*1,
     $   6*1,12*2,1,1,2,2,3*1,2,1,2,18*1,21*2,9*1,
     $   5*1,14*2,6*1,2,2,19*1,2,1,18*2,10*1,
     $   8*1,11*2,7*1,2,20*1,2,2,1,17*2,9*1,
     $   6*1,2,1,10*2,30*1,18*2,10*1,6*1,14*2,28*1,18*2,10*1,
     $   8*1,10*2,1,2,28*1,2,2,1,14*2,11*1,
     $   8*1,9*2,1,3*2,27*1,3*2,1,13*2,11*1,
     $   1,1,2,4*1,11*2,1,2,2,1,2,24*1,3*2,1,1,12*2,10*1,2,1,
     $   1,1,2,3*1,12*2,1,3*2,1,2,24*1,3*2,1,12*2,10*1,2,1,
     $   3*2,1,1,15*2,4*1,2,25*1,2,1,6*2,14*1,3*2,1,
     $   1,2,2,1,5*2,1,1,9*2,3*1,2,31*1,3*2,15*1,2,2,1,
     $   1,2,2,1,1,4*2,1,1,3*2,1,1,5*2,1,1,2,1,1,2,28*1,4*2,14*1,2,2,1 =
     $   4*1,2,1,1,2,2,3*1,3*2,1,1,5*2,5*1,2,48*1,
     $   6*1,3*2,5*1,8*2,5*1,2,2,25*1,4*2,18*1,
     $   1,2,4*1,3*2,6*1,9*2,1,6*2,1,2,18*1,8*2,8*1,2,3*1,2,1,2,1,1,
     $   2,4*1,3*2,7*1,14*2,1,3*2,12*1,23*2,1,1,3*2,3*1/
      WRITE(LOUT,10) LANSEA
```

PROGRAM PAXXPAXX/MAIN

```
 CCMMON
$/XXXXIO/ LWIND,LLAND,LPROP,LOUT,LARCH1,LARCH2,LRST1,LRST2,
$   LSCR1,LSCR2,RUNID
$/XXTIME/ KSTEP1,KSTEP2,KSTEP3,ISTEP,DELT,DELTAH,YMDH,ZMDH,
$   LSKIP,KDT
$/XSPEC1/ SPOLD(280,76,3)
$/XSPEC2/ SPNEW(280,76)
$/XPARAM/ CA,CB,FREQ1,FREQ2,WEDGE,DIREC(20),COSS(2,10),
$   DELOG,OMEGA(2,14),FREQ(14),DOM(14),RBW(14),OMM4(14),
$   OM3DD(14),OM116(14),OM25(14),DOMM4(14),OMK(14)
$/XXGRID/ LAT,LONG,KPCINT
$/XXLAND/ LANSEA(76,73)
$/XXWIND/ WIND(2,76,73)
$/XXXH13/ FRONT(4),H13(76,73)
$/XXPROP/ JPROP(13,280,73),PROP(6,280,73)
$/XXPACK/ EEE(76),SPEC16(280,76)
 INTEGER*2 SPEC16
 INTEGER*4 DELTAH,RUNID,YMDH,ZMDH
 INTEGER*2 LANSEA,JPROP
 CALL WWORK
 STOP
 END
```

```
      SUBROUTINE WWORK
      COMMON
     $/XXXXIO/ LWIND,LLAND,LPROP,LOUT,LARCH1,LARCH2,LRST1,LRST2,
     $  LSCR1,LSCR2,RUNID
     $/XXTIME/ KSTEP1,KSTEP2,KSTEP3,ISTEP,DELT,DELTAH,YMDH,ZMDH,
     $  LSKIP,KBT
     $/XPARAM/ CA,CB,FREQ1,FREQ2,WEDGE,DIREC(20),COSS(2,10),
     $  DELOG,OMEGA(2,14),FREQ(14),DOM(14),RBW(14),OMM4(14),
     $  OM3DD(14),OM116(14),OM25(14),DOMM4(14),OMK(14)
     $/XXLAND/ LANSEA(76,73)
     $/XXWIND/ WIND(2,76,73)
     $/XXPROP/ JPROP(13,280,73),PROP(6,280,73)
      INTEGER*4 DELTAH,RUNID,YMDH,ZMDH
      INTEGER*2 LANSEA,JPROP
      NAMELIST /WHAT/ LWIND,LLAND,LPROP,LOUT,LARCH1,LARCH2,
     $  LRST1,LRST2,LSCR1,LSCR2,KSTEP1,KSTEP2,KSTEP3,YMDH,LSKIP,KBT,
     $  CA,CB,RUNID
      DATA LIN/5/
      LWIND = 10
      LLAND = 11
      LPROP = 12
      LOUT = 6
      LARCH1 = 13
      LARCH2 = 14
      LRST1 = 15
      LRST2 = 16
      LSCR1 = 17
      LSCR2 = 18
      KSTEP1 = 1
      KSTEP2 = 0
      KSTEP3 = 32767
      DELT = 5400.
      DELTAH = 3
      YMDH = -1
      LSKIP = 0
      KBT = 1
      CA = 1.36E-9
      CB = .1066
      FREQ1 = .04
      FREQ2 = .20
      WEDGE = 18.
      READ (LIN,WHAT)
      WRITE (LOUT,WHAT)
      IF (LWIND .LE. 0) STOP 354
      IF (LLAND .LE. 0) STOP 355
      IF (LPROP .LE. 0) STOP 356
      IF (LOUT .LE. 0) STOP 357
      IF (LOUT .EQ. LWIND) STOP 357
      IF (LOUT .EQ. LLAND) STOP 357
      IF (LOUT .EQ. LPROP) STOP 357
      IF (LARCH1 .LE. 0) STOP 360
      IF (LARCH1 .EQ. LWIND) STOP 360
      IF (LARCH1 .EQ. LLAND) STOP 360
      IF (LARCH1 .EQ. LPROP) STOP 360
      IF (LARCH1 .EQ. LOUT) STOP 360
      IF (LARCH2 .LE. 0) STOP 361
      IF (LARCH2 .EQ. LWIND) STOP 361
      IF (LARCH2 .EQ. LLAND) STOP 361
      IF (LARCH2 .EQ. LPROP) STOP 361
      IF (LARCH2 .EQ. LOUT) STOP 361
      IF (LRST1 .LE. 0) STOP 362
      IF (LRST1 .EQ. LWIND) STOP 362
      IF (LRST1 .EQ. LLAND) STOP 362
      IF (LRST1 .EQ. LPROP) STOP 362
      IF (LRST1 .EQ. LOUT) STOP 362
```

```
      IF (LRST1 .EQ. LARCH1) STOP 362
      IF (LRST1 .EQ. LARCH2) STOP 362
      IF (LRST2 .LE. 0) STOP 363
      IF (LRST2 .EQ. LWIND) STOP 363
      IF (LRST2 .EQ. LLAND) STOP 363
      IF (LRST2 .EQ. LPROP) STOP 363
      IF (LRST2 .EQ. LOUT) STOP 363
      IF (LRST2 .EQ. LARCH1) STOP 363
      IF (LRST2 .EQ. LARCH2) STOP 363
      IF (LSCR1 .LE. 0) STOP 364
      IF (LSCR1 .EQ. LWIND) STOP 364
      IF (LSCR1 .EQ. LLAND) STOP 364
      IF (LSCR1 .EQ. LPROP) STOP 364
      IF (LSCR1 .EQ. LOUT) STOP 364
      IF (LSCR1 .EQ. LARCH1) STOP 364
      IF (LSCR1 .EQ. LARCH2) STOP 364
      IF (LSCR2 .LE. 0) STOP 365
      IF (LSCR2 .EQ. LWIND) STOP 365
      IF (LSCR2 .EQ. LLAND) STOP 365
      IF (LSCR2 .EQ. LPROP) STOP 365
      IF (LSCR2 .EQ. LOUT) STOP 365
      IF (LSCR2 .EQ. LARCH1) STOP 365
      IF (LSCR2 .EQ. LARCH2) STOP 365
      IF (LSCR2 .EQ. LRST1) STOP 365
      IF (LSCR2 .EQ. LRST2) STOP 365
      IF (LSCR2 .EQ. LSCR1) STOP 365
      IF (KSTEP1 .LE. 0) STOP 366
      IF (KSTEP2 .LT. KSTEP1) STOP 367
      IF (KSTEP2 .GT. 32767) STOP 367
      IF (KSTEP3 .LE. 0) STOP 370
      IF (YMDH .LE. 0) STOP 371
      IF (MOD(YMDH,100).GT. 23) STOP 371
      KA = MOD(YMDH,10000)
      IF (KA .EQ. 0) STOP 371
      IF (KA .GT. 3123) STOP 371
      KA = MOD(YMDH,1000000)
      IF (KA .EQ. 0) STOP 371
      IF (KA .GT. 123123) STOP 371
      IF (YMDH .GT. 99123123) STOP 371
      IF (LSKIP .LT. 0) STOP 372
      IF (LSKIP .GE. 32767) STOP 372
      IF (KBT .LT. 0) STOP 373
      IF (KBT .GT. 1) STOP 373
      IF (CA .LE. 0) STOP 374
      IF (CB .LE. 0) STOP 375
      CALL BREW (LRST1)
C ACQUIRE LAND-SEA TABLE
      CALL BREW (LLAND)
      CALL BREAD2 (LLAND,LANSEA,5548)
C ACQUIRE INITIAL WIND FIELD
      IF (LWIND .NE. LLAND) CALL BREW (LWIND)
      MSKIP = LSKIP+1
      DO 381 IA = 1,MSKIP
        CALL BREAD4 (LWIND,WIND,11096)
381   CONTINUE
C SET DATE AND TIME
      ZMDH = YMDH
      IF (KSTEP1 .EQ. 1) GO TO 387
      DO 386 IA = 2,KSTEP1
        CALL BUMP
386   CONTINUE
387   CALL LODTAB
C ACQUIRE PROPAGATE TABLES
      IF (LPROP .NE. LLAND) CALL BREW (LPROP)
      CALL BREAD2 (LPROP,JPROP,265720)
      CALL BREAD4 (LPROP,PROP,122640)
      DO 396 IA = KSTEP1,KSTEP2
        ISTEP = IA
        CALL WWAX1
        CALL BUMP
        CALL ORWAX2
396   CONTINUE
      RETURN
```

```
      SUBROUTINE LODTAB
      COMMON
     $/XXTIME/ KSTEP1,KSTEP2,KSTEP3,ISTEP,DELT,DELTAH,YMDH,ZMDH,
     $  LSKIP,KBT
     $/XPARAM/ CA,CB,FREQ1,FREQ2,WEDGE,DIREC(20),COSS(2,10),
     $  DELOG,OMEGA(2,14),FREQ(14),DOM(14),RBW(14),OMM4(14),
     $  OM3DD(14),OM116(14),OM25(14),DOMM4(14),OMK(14)
      NAMELIST /TABS/DIREC,COSS,OMEGA,FREQ,DOM,RBW,OMM4,OM3DD,
     $OM116,OM25,DOMM4,OMK
      DO 419 IA = 1,20
        DIREC(IA) = 18*IA-9
419   CONTINUE
      DO 425 IA = 1,10
        BB = .31415926*FLOAT(IA-1)
        COSS(1,IA) = COS(BB)
        COSS(2,IA) = SIN(BB)
425   CONTINUE
      DELOG = .08*ALOG(5.)
      OMEGA(1,1) = .015625
      OMEGA(2,1) = 6.2831853*FREQ1
      BB = EXP(.5*DELOG)
      DO 432 IA = 3,28
        OMEGA(IA,1) = BB*OMEGA(IA-1,1)
432   CONTINUE
      DO 435 IA = 1,14
        FREQ(IA) = OMEGA(2,IA)/6.2831853
435   CONTINUE
      DO 438 IA = 2,13
        DOM(IA) = OMEGA(1,IA+1)-OMEGA(1,IA)
438   CONTINUE
      DOM(1) = DOM(2)
      DOM(14) = .25/OMEGA(1,14)**4*OMEGA(2,14)**5
      BACA = .314159265*CA
      DO 449 IA = 1,14
        RBW(IA) = 6.2831853/DOM(IA)
        OMM4(IA) = OMEGA(1,IA)**(-4)
        OM3DD(IA) = BACA*OMEGA(2,IA)**3*DOM(IA)
        OM116(IA) = OMEGA(2,IA)**1.16
        OM25(IA) = OMEGA(2,IA)**(-2.5)
        OMK(IA) = OMEGA(2,IA)**2/9.806
449   CONTINUE
      DO 452 IA = 1,13
        DOMM4(IA) = OMM4(IA)-OMM4(IA+1)
452   CONTINUE
      DOMM4(14) = OMM4(14)
      DO 456 IA = 1,14
        DOMM4(IA) = DOMM4(IA)*24.039409
456   CONTINUE
C 24.039409 = 9.806**2/4
      WRITE(6,TABS)
      RETURN
      END
```

```
      SUBROUTINE WWAX1
      COMMON /XXXXIO/ LWIND,LLAND,LPROP,LOUT,LARCH1,LARCH2,LRST1,_RS
     $  LSCR1,LSCR2,RUNID /XXTIME/ KSTEP1,KSTEP2,KSTEP3,ISTEP,DELT,
     $  DELTAH,YMDH,ZMDH,LSKIP,KBT /XXPACK/ EEE(76),SPEC16(280,76)
     $/XSPEC2/ SPNEW(280,76) /XXGRID/ LAT,LONG,KPOINT /XXLAND/
     $  LANSEA(76,73) /XXWIND/ WIND(2,76,73)
      INTEGER*2 SPEC16,LANSEA
      LOGICAL DEADST
      DEADST = (ISTEP .EQ. 1)
      CALL BREW (LSCR1)
      CALL BREW (LSCR2)
      IF (MOD(ISTEP,2).EQ. 0 .AND. ISTEP .NE. KSTEP1)
     $  CALL BREAD4 (LWIND,WIND,11096)
      DO 820 LLAT = 1,73
        LAT = LLAT
        IF (DEADST) GO TO 811
        CALL BREAD4 (LSCR1,EEE,76)
        CALL BREAD2 (LSCR1,SPEC16,21280)
        CALL UNPACO
        GO TO 813
811     DO 812 IA = 1,21280
          SPNEW(IA,1) = 0.
812     CONTINUE
813     DO 814 LLONG = 3,74
          LONG = LLONG
          IF (LANSEA(LLONG,LLAT).EQ. 2) CALL CMPE27
814     CONTINUE
        CALL PACO
        EEE(1) = EEE(73)
        EEE(2) = EEE(74)
        EEE(75) = EEE(3)
        EEE(76) = EEE(4)
        DO 815 IA = 1,560
          SPEC16(IA,1) = SPEC16(IA,73)
          SPEC16(IA,75) = SPEC16(IA,3)
815     CONTINUE
        CALL BRITE4 (LSCR2,EEE,76)
        CALL BRITE2 (LSCR2,SPEC16,21280)
820   CONTINUE
      RETURN
      END
```

```
      SUBROUTINE CMPE27
C REFERENCE SPECTRUM BASED ON U(19.5)**4
      COMMON
     $/XXTIME/ KSTEP1,KSTEP2,KSTEP3,ISTEP,DELT,DELTAH,YMDH,ZMDH,
     $  LSKIP,KBT
     $/XSPEC2/ SPNEW(14,20,76)
     $/XPARAM/ CA,CB,FREQ1,FREQ2,WEDGE,DIREC(20),COSS(2,10),
     $  DELOG,OMEGA(2,14),FREQ(14),DOM(14),RBW(14),OMM4(14),
     $  OM3DD(14),OM116(14),OM25(14),DOMM4(14),OMK(14)
     $/XXGRID/ LAT,LONG,KPCINT
     $/XXLAND/ LANSEA(76,73)
     $/XXWIND/ WIND(2,76,73)
C    $//  DE,EX,OMSPEC,PMSPEC,SPREAD,TRIG
      INTEGER*2 LANSEA
      REAL*4 UXMULT(68),UKAPPA(68),GAMMAK(75),DELTAK(75)
      DATA UXMULT/
     $  .033459130,.032905749,.032705244,.032782464,.033070655,
     $  .033505080,.034030014,.034604220,.035200157,.035801416,
     $  .036398469,.036986276,.037562479,.038126069,.038676973,
     $  .039215548,.039742369,.040258113,.040763505,.041259258,
     $  .041746046,.042224514,.042695259,.043158832,.043615745,
     $  .044066470,.044511437,.044951047,.045385666,.045815635,
     $  .046241270,.046662858,.047080670,.047494955,.047905950,
     $  .048313869,.048718919,.049121290,.049521158,.049918700,
     $  .050314064,.050707404,.051098861,.051488571,.051876658,
     $  .052263245,.052648445,.053032369,.053415122,.053796804,
     $  .054177510,.054557336,.054936363,.055314681,.055692370,
     $  .056069509,.056446177,.056822446,.057198388,.057574074,
     $  .057949569,.058324942,.058700256,.059075572,.059450952,
     $  .059826457,.060202149,.060578078/
      DATA UKAPPA/
     $  1.11959678,1.08116600,1.05961519,1.04698433,1.03938176,
     $  1.03457963,1.03125800,1.02865642,1.02636987,1.02418266,
     $  1.02199487,1.01976140,1.01746383,1.01510145,1.01267745,
     $  1.01019831,1.00767146,1.00510420,1.00250289, .99987330,
     $   .99722051, .99454892, .99186222, .98916370, .98645602,
     $   .98374152, .98102220, .97829975, .97557563, .97285104,
     $   .97012699, .96740442, .96468406, .96196653, .95925236,
     $   .95654205, .95383593, .95113428, .94843744, .94574545,
     $   .94305868, .94037717, .93770193, .93503022, .93236195,
     $   .92970514, .92705081, .92440198, .92175855, .91912054,
     $   .91648787, .91386045, .91123831, .90862127, .90600933,
     $   .90340237, .90080024, .89820291, .89561024, .89302212,
     $   .89043847, .88785915, .88528406, .88271305, .88014607,
     $   .87758294, .87502354, .87246776/
      DATA GAMMAK/
     $  .13711098,.15359526,.16647946,.17721295,.18640458,.19472033,
     $  .20213850,.20891603,.21517106,.22099060,.22644076,.23157303,
     $  .23642843,.24104016,.24543554,.24963734,.25366477,.25753417,
     $  .26125960,.26485322,.26832566,.27168624,.27494321,.27810388,
     $  .28117480,.28416180,.28707019,.28990472,.29266973,.29536914,
     $  .29800658,.30058531,.30310838,.30557857,.30799847,.31037043,
     $  .31269667,.31497925,.31722006,.31942090,.32158342,.32370918,
     $  .32579964,.32785617,.32988004,.33187249,.33383464,.33576757,
     $  .33767232,.33954982,.34140100,.34322672,.34502781,.34680504,
     $  .34855916,.35029086,.35200083,.35368970,.35535809,.35700656,
     $  .35863570,.36024603,.36183806,.36341228,.36496915,.36650913,
     $  .36803265,.36954012,.37103195,.37250850,.37397016,.37541727,
     $  .37685019,.37826923,.37967470/
      DATA DELTAK/
     $  .75663491,.74060861,.72944406,.72090019,.71399369,.70820597,
     $  .70323035,.69887057,.69499353,.69150484,.68835522,.68543228,
     $  .68275549,.68027285,.67795867,.67579202,.67375558,.67183491,
     $  .67001786,.66829403,.66665454,.66509171,.66359881,.66217004,
     $  .66080020,.65948474,.65821961,.65700117,.65582620,.65469175,
```

```
     $   .65359518,.65253412,.65150639,.65050999,.64954312,.64860413,
     $   .64769148,.64680378,.64593972,.64509811,.64427784,.64347788,
     $   .64269727,.64193512,.64119060,.64046292,.63975137,.63905526,
     $   .63837394,.63770681,.63705332,.63641293,.63578513,.63516946,
     $   .63456546,.63397272,.63339081,.63281938,.63225806,.63170649,
     $   .62116437,.63063139,.63010703,.62959162,.62908430,.62858501,
     $   .62809349,.62760952,.62713291,.62666338,.62620077,.62574489,
     $   .62529554,.62485252,.62441569/
      REAL*4 KAPPA,KAPPA1
      REAL*4 EX(20),DE(20)
      REAL*4 TRIG(20,3),OMSPEC(14),PMSPEC(14,2),SPREAD(14,20,2)
      ALPHA(X) = .0081/X**.23
      COCS(X) = (3.8663239E-9*X-1.5230871E-4)*X+1.
      SIIN(X) = (1.3496016E-11*X-6.8609616E-7)*X+.017453293
C N.B.  THESE FORMULAS GOOD FOR ND .GE. 16
C ACQUIRE USTAR AND THETA SUB W
      XSPEED = WIND(1,LONG,LAT)-2.11
      IF (XSPEED .LT. 1.) GO TO 675
      KSPEED = XSPEED
C     IF (KSPEED .EQ. 0.) GO TO 675
      IF (KSPEED .GE. 68) GO TO 494
      XSPEED = XSPEED-AINT(XSPEED)
      YSPEED = 1.-XSPEED
      UX = WIND(1,LONG,LAT)*
     $   (YSPEED*UXMULT(KSPEED)+XSPEED*UXMULT(KSPEED+1))
      KAPPA1 = (YSPEED*UKAPPA(KSPEED)+XSPEED*UKAPPA(KSPEED+1))/
     $   WIND(1,LONG,LAT)
      GO TO 496
494   UX = WIND(1,LONG,LAT)*UXMULT(68)
      KAPPA1 = UKAPPA(68)/WIND(1,LONG,LAT)
496   THW = WIND(2,LONG,LAT)+180.
      IF (THW .GE. 360.) THW = THW-360.
C     WRITE(6,10) CA,CB,FREQ1,FREQ2,WEDGE,(DIREC(I),I=1,20)
C 010 FORMAT(/1X,'CA=',F10.2,2X,'CB=',F10.2,2X,'FREQ1=',F10.2,2X,
C    $'FREQ2=',F10.2,2X,'WEDGE=',F4.2/1X,'DIREC=',10(F10.2,2X))
      KTH = THW/WEDGE
      IF (KTH .EQ. 20) KTH = 0
C COMPUTE COS(THETA BAR - THETA W), ETC.
C     DO 1 IT=1,10
C     WRITE(6,2) IT,COSS(1,IT),COSS(2,IT)
C 002 FORMAT(/1X,'IT=',I2,2X,'COSS(1,IT)=',F8.2,2X,'COSS(2,IT)=',
C    $F8.2)
C 001 CONTINUE
      DO 503 IA = 1,20
        TRIG(IA,1) = 0.
503   CONTINUE
      KA = KTH
      ANG = THW-DIREC(KTH+1)
      ANG2 = ANG**2
      CAA = COCS(ANG2)
      SA = SIIN(ANG2)*ANG
C     WRITE(6,3) KTH,ANG,ANG2,CAA,SA
C 003 FORMAT(/1X,'KTH=',F8.2,2X,'ANG=',F8.2,2X,'ANG2=',F8.2,2X,
C    $'CAA=',F8.2,2X,'SA=',F8.2)
      DO 513 IA = 1,10
        KA = KA+1
        IF (KA .EQ. 21) KA = 1
        TRIG(KA,1) = COSS(1,IA)*CAA+COSS(2,IA)*SA
513   CONTINUE
      DO 4 IT=1,20
C     WRITE(6,7) IT,TRIG(IT,1),TRIG(IT,2),TRIG(IT,3)
C 007 FORMAT(/1X,'IT=',I2,2X,'TRIG(IT,1)=',F10.2,2X,'TRIG(IT,2)=',
C    $F10.2,2X,'TRIG(IT,3)=',F10.2)
  004 CONTINUE
      KA = 10
      DO 521 IA = 1,20
        KA = KA+1
        IF (KA .EQ. 21) KA = 1
        IF (TRIG(IA,1).EQ. 0.) TRIG(IA,1) = -TRIG(KA,1)
        TRIG(IA,2) = TRIG(IA,1)**2
        IF (TRIG(IA,1).GT. 0.) TRIG(IA,2) = 1.-TRIG(IA,2)
521   CONTINUE
C COMPUTE OMEGA ZERO AND OMEGA PEAK
```

```
      OMO = (.92748721*9.806)/WIND(1,LONG,LAT)
C .92748721 = .74**.25
      OMPEAK = .94574161*OMO
C COMPUTE TOTAL ENERGY
      ED = 0.
      DO 530 IA = 1,280
        ED = ED+SPNEW(IA,1,LONG)
530   CONTINUE
      UX4 = UX**4
      OMOA = OMO**4
      GUX4 = OM04/(.0081*.25*9.806*9.806)
      UG = UX/9.806
C COMPUTE REFERENCE SPECTRUM
      DO 540 IA = 2,14
        PMSPEC(IA,1) = 0.
        BA = OM04*OMM4(IA)
        IF (BA .LT. 88.) PMSPEC(IA,1) = EXP(-BA)
540   CONTINUE
      BA = (.25*9.806*9.806)/OM04
      PMSPEC(1,2) = BA*PMSPEC(2,1)
      DO 545 IA = 3,14
        PMSPEC(IA-1,2) = BA*(PMSPEC(IA,1)-PMSPEC(IA-1,1))
545   CONTINUE
      PMSPEC(14,2) = BA*(1.-PMSPEC(14,1))
      OMP25 = OMPEAK**2.5
      DO 572 IA = 1,14
        S = OMP25*OM25(IA)
        IF (S .GT. 1.) S = 1./S**2
        S = 15.00496*S
        KS = S
        IF (KS .NE. 0) GO TO 559
        DO 557 IB = 1,20
          TRIG(IB,3) = 0.
          IF (TRIG(IB,1).GT. 0.) TRIG(IB,3) = TRIG(IB,1)
557     CONTINUE
        GO TO 565
559     XS = S-AINT(S)
        DO 564 IB = 1,20
          TRIG(IB,3) = 0.
          IF (TRIG(IB,1).GT. 0.)
     *      TRIG(IB,3) = (1.+TRIG(IB,1))**KS*(1.+XS*TRIG(IB,1))-1.
564     CONTINUE
565     BA = 0.
        DO 568 IB = 1,20
          BA = BA+TRIG(IB,2)
568     CONTINUE
        DO 571 IB = 1,20
          SPREAD(IA,IB,2) = PMSPEC(IA,2)*TRIG(IB,3)/BA
571     CONTINUE
572   CONTINUE
C CYCLE THROUGH FREQUENCIES
      DO 674 IA = 1,14
C CALCULATE ALPHA
        AL = 1.
      IF(ED.GT.0.) AL=ALPHA(ED*GUX4)
        OMSPEC(IA) = 0.
        DO 580 IB = 1,20
          OMSPEC(IA) = OMSPEC(IA)+SPNEW(IA,IB,LONG)
580     CONTINUE
C     WRITE(6,20) AL,ED,OMSPEC,(SPNEW(IA,IB,LONG),IB=1,20)
C 020 FORMAT(/1X,'AL=',F10.1,2X,'ED=',F10.1,2X,
C    *,/1X,'OMSPEC=',F10.1,/1X,'SPNEW=',10(F10.1,2X))
        ED = ED-OMSPEC(IA)
C CUT BACK HIGH FREQUENCIES
        CUT = AL*DOMM4(IA)
        IF (OMSPEC(IA).LE. CUT) GO TO 589
        CUT = CUT/OMSPEC(IA)
C     WRITE(6,21) ED,CUT,DOMM4
C 021 FORMAT(/1X,'ED=',F10.1,2X,'CUT=',F10.1,2X,'DOMM4=',F10.1)
        DO 588 IB = 1,20
          SPNEW(IA,IB,LONG) = SPNEW(IA,IB,LONG)*CUT
588     CONTINUE
C     WRITE(6,22) CUT,(SPNEW(IA,IB,LONG),IB=1,20)
```

```
C 022 FORMAT(/1X,'CUT=',F10.1,2X,'SPNEW=',10(F10.1,1X))
589      CONTINUE
C DISSIPATE OPPOSING BANDS
         DO 598 IB = 1,10
           IF (SPNEW(IA,IB,LONG).EQ. 0.) GO TO 598
           IF (SPNEW(IA,IB+10,LONG).EQ. 0.) GO TO 598
           BA = ABS(SPNEW(IA,IB,LONG)-SPNEW(IA,IB+10,LONG))/
     $       (SPNEW(IA,IB,LONG)+SPNEW(IA,IB+10,LONG))
           SPNEW(IA,IB,LONG) = SPNEW(IA,IB,LONG)*BA
           SPNEW(IA,IB+10,LONG) = SPNEW(IA,IB+10,LONG)*BA
598      CONTINUE
C COMPUTE DOWNWIND ENERGY IN FREQUENCY BAND
         BA = 0.
         DO 606 IB = 1,20
           IF (TRIG(IB,1)) 606,603,605
603        BA = BA+.5*SPNEW(IA,IB,LONG)
           GO TO 606
605        BA = BA+SPNEW(IA,IB,LONG)
606      CONTINUE
C IF UNDERDEVELOPED GROW. IF OVERDEVELOPED, REDISTRIBUTE.
         IF (BA .GE. AL*PMSPEC(IA,2)) GO TO 647
C GROW
         PSI = OMEGA(2,IA)*UG
         KAPPA = KAPPA1*OMI16(IA)
         XKAPPA = KAPPA*100.-1.
         KKAPPA = XKAPPA
         IF (KKAPPA .GT. 0) GO TO 618
         GAMMA = .0027422197
         DELTA = .0151326985
         GO TO 622
618      XKAPPA = XKAPPA-AINT(XKAPPA)
         YKAPPA = 1.-XKAPPA
         GAMMA = KAPPA*(YKAPPA*GAMMAK(KKAPPA)+XKAPPA*GAMMAK(KKAPPA+1
         DELTA = KAPPA*(YKAPPA*DELTAK(KKAPPA)+XKAPPA*DELTAK(KKAPPA+1
622      ANUM = UX4*OM3DD(IA)
         DO 644 IB = 1,20
           IF (TRIG(IB,1).LE. 0.) GO TO 644
           SPREAD(IA,IB,1) = AL*SPREAD(IA,IB,2)
           IF (SPNEW(IA,IB,LONG).GE. SPREAD(IA,IB,1)) GO TO 644
           PSII = PSI*TRIG(IB,1)
           BX = CB*(PSII**2-.0004)
       IF(KBT.NE.0.)
     $       EX = BX+CB/(503.3+(2042E3+12203E4*PSII)*(PSII-.031)**2)
           IF (BX .LE. 0.) GO TO 644
           BT = BX*OMEGA(2,IA)
           BDT = BT*DELT
           IF (BDT .LT. 77.) GO TO 637
           SPNEW(IA,IB,LONG) = SPREAD(IA,IB,1)
           GO TO 644
637        AT = ANUM/
     $       ((GAMMA+(OMK(IA)*TRIG(IB,1)-KAPPA)**2/GAMMA)*
     $       (DELTA+OMK(IA)**2*TRIG(IB,2)/DELTA))
           AB = AT/BT
           SPNEW(IA,IB,LONG) = (SPNEW(IA,IB,LONG)+AB)*EXP(BDT)-AB
           IF (SPNEW(IA,IB,LONG).GT. SPREAD(IA,IB,1))
     $       SPNEW(IA,IB,LONG) = SPREAD(IA,IB,1)
644      CONTINUE
         GO TO 669
C REDISTRIBUTE OVER ANGLES
647      SX = 0.
         SY = 0.
         DO 660 IB = 1,20
           EX(IB) = 0.
           DE(IB) = 0.
           IF (TRIG(IB,1).LE. 0.) GO TO 660
           BB = SPNEW(IA,IB,LONG)-AL*SPREAD(IA,IB,2)
           IF (BB) 655,660,658
655        DE(IB) = -BB
           SY = SY-BB
           GO TO 660
658        EX(IB) = BB
           SX = SX+BB
660      CONTINUE
```

```
      IF (SX .EQ. 0.) GO TO 669
      IF (SY .EQ. 0.) GO TO 669
      RAT1 = SX/BA
      RAT2 = RAT1*SX/SY
      DO 668 IB = 1,20
        IF (TRIG(IB,1).GT. 0.)
     $     SPNEW(IA,IB,LONG) =
     $     SPNEW(IA,IB,LONG)-RAT1*EX(IB)+RAT2*DE(IB)
668   CONTINUE
669   CMSPEC(IA) = 0.
      DO 672 IB = 1,20
        CMSPEC(IA) = CMSPEC(IA)+SPNEW(IA,IB,LONG)
672   CONTINUE
    ED = ED+CMSPEC(IA)
674 CONTINUE
675 CONTINUE
C COMPUTE EPS
    ED = 0.
    DO 680 IA = 1,280
      ED = ED+SPNEW(IA,1,LONG)
680 CONTINUE
    EPS = ED*GUX4
    RETURN
    END
```

```
      SUBROUTINE ORWAX2
      COMMON /XXPACK/ EEE(76),SPEC16(280,76) /XXXX10/ LWIND,LLAND,LPROP,
     $  LOUT,LARCH1,LARCH2,LRST1,LRST2,LSCR1,LSCR2,RUNID /XXTIME/ KSTEP1
     $  ,KSTEP2,KSTEP3,ISTEP,DELT,DELTAH,YMDH,ZMDH,LSKIP,KBT /XSPEC1/
     $  SPOLD(280,76,3) /XSPEC2/ SPNEW(280,76) /XXGRID/ LAT,LONG,KPOINT
     $/XXLAND/ LANSEA(76,73) /XXWIND/ WIND(2,76,73) /XXXH13/ JFRONT(4),
     $  H13(76,73) /XXPROP/ JPROP(13,280,73),PROP(6,280,73)
      INTEGER*4 DELTAH,RUNID,YMDH,ZMDH
      INTEGER*2 LANSEA,JPROP,MOOD(73),SPEC16
      DATA MOOD/3,1,2,3,1,2,3,1,2,3,1,2,3,1,2,3,1,2,3,1,2,3,1,2,3,
     $  1,2,3,1,2,3,1,2,3,1,2,3,1,2,3,1,2,3,1,2,3,1,2,3,1,2,3,1,2,
     $3,1,2,3,1,2,3,1,2,3,1,0,0/
      JFRONT(1) = RUNID
      JFRONT(2) = ISTEP
      JFRONT(3) = ZMDH
      JFRONT(4) = MOD(ISTEP,KSTEP3)
      IF (JFRONT(4).EQ. 0) CALL BRITE4 (LARCH1,JFRONT,3)
      CALL BREW (LSCR1)
      CALL BREW (LSCR2)
      CALL BREAD4 (LWIND,WIND,11096)
      DO 822 IA = 1,5548
        H13(IA,1) = 0.
822   CONTINUE
      CALL GRAB(1)
      CALL GRAB(2)
      DO 830 LLAT = 1,73
        LAT = LLAT
        MLAT = MOOD(LLAT)
        CALL GRAB (MLAT)
        DO 823 IA = 1,21280
          SPNEW(IA,1) = 0.
823     CONTINUE
        DO 827 LLONG = 3,74
          IF (LANSEA(LLONG,LLAT).NE. 2) GO TO 827
          LONG = LLONG
          KPOINT = 76*LLAT+LLONG
          DO 825 IA = 1,280
            KPART = JPROP(1,IA,LLAT)
            IF (KPART .EQ. 0) GO TO 825
            DO 824 IB = 1,KPART
              KB = KPOINT+JPROP(2*IB,IA,LLAT)
              IF (LANSEA(KB-76,1).NE. 2) GO TO 824
              KC = IA+JPROP(2*IB+1,IA,LLAT)+21280
              SPNEW(IA,LLONG) = SPNEW(IA,LLONG)+
     $          SPOLD(KC,LLONG,1)*PROP(IB,IA,LLAT)
824         CONTINUE
825       CONTINUE
          CALL CMPE27
          EE = 0.
          DO 826 IA = 1,280
            EE = EE+SPNEW(IA,LLONG)
826       CONTINUE
          H13(LLONG,LLAT) = 4.*SQRT(EE)
827     CONTINUE
        CALL PAOQ
        IF (JFRONT(4).NE. 0) GO TO 828
        CALL BRITE4 (LARCH1,EEE,76)
        CALL BRITE2 (LARCH1,SPEC16,21280)
828     CALL BRITE4 (LSCR1,EEE,76)
        CALL BRITE2 (LSCR1,SPEC16,21280)
830   CONTINUE
        CALL BRITE4 (LARCH2,JFRONT,5552)
      IF (JFRONT(4).EQ. 0) CALL BEND (LARCH1)
      WRITE(6,831) JFRONT,((I,J,H13(J,I),J=3,74),I=1,73)
  831 FORMAT(1H1,4I10//(9(I4,I3,F7.3)))
```

```
      SUBROUTINE GRAB (I)
      COMMON /XSPEC1/ SPOLD(280,76,3) /XSPEC2/ SPNEW(280,76)
     $/XXPACK/ EEE(76),SPEC16(280,76)
      COMMON
     $/XXXXIO/ LWIND,LLAND,LPROP,LOUT,LARCH1,LARCH2,LRST1,LRST2,
     $  LSCR1,LSCR2,RUNID
      INTEGER*2 SPEC16
      IF (I .EQ. 0) RETURN
      CALL BREAD4 (LSCR2,EEE,76)
      CALL BREAD2 (LSCR2,SPEC16,21280)
      CALL UNPAQQ
      DO 821 IA = 1,21280
        SPOLD(IA,1,I) = SPNEW(IA,1)
821   CONTINUE
      RETURN
      END
```

```
      SUBROUTINE PACK
      COMMON /XSPEC2/ SPNEW(280,76) /XXPACK/ EEE(280),SPEC16(280,76)
      INTEGER*2 SPEC16
      DO 805 IA = 1,76
        EEE(IA) = 0.
        DO 800 IB = 1,280
          IF (SPNEW(IB,IA).GT. EEE(IA)) EEE(IA) = SPNEW(IB,IA)
800     CONTINUE
        IF (EEE(IA).GT. 0.) GO TO 802
        DO 801 IB = 1,280
          SPEC16(IB,IA) = 0
801     CONTINUE
        GO TO 805
802     BA = 32767./EEE(IA)
        DO 803 IB = 1,280
          SPEC16(IB,IA) = BA*SPNEW(IB,IA)+.5
803     CONTINUE
805   CONTINUE
      RETURN
      END
```

```
      SUBROUTINE UNPAQQ
      COMMON /XSPEC2/ SPNEW(280,76) /XXPACK/ EEE(280),SPEC16(280,76)
      INTEGER*2 SPEC16
      DO 810 IA = 1,76
        IF (EEE(IA).EQ. 0.) GO TO 807
        BB = EEE(IA)/32767.
        DO 806 IB = 1,280
          BC=SPEC16(IB,IA)
          SPNEW(IB,IA) = BB*BC
806     CONTINUE
        GO TO 810
807     DO 808 IB = 1,280
          SPNEW(IB,IA) = 0.
808     CONTINUE
810   CONTINUE
      RETURN
      END
```

```
SUBROUTINE BREAD2 (LU,ARRAY,NPOINT)
INTEGER*2 ARRAY(NPOINT)
READ (LU) ARRAY
RETURN
END
```

```
      SUBROUTINE BREAD4 (LU,ARRAY,NPOINT)
      INTEGER*4 ARRAY(NPOINT)
      READ (LU) ARRAY
      RETURN
      END
```

```
SUBROUTINE BRITE2 (LU,ARRAY,NPOINT)
INTEGER*2 ARRAY(NPOINT)
WRITE (LU) ARRAY
RETURN
END
```

```
SUBROUTINE BRITE4 (LU,ARRAY,NPOINT)
INTEGER*4 ARRAY(NPOINT)
WRITE (LU) ARRAY
RETURN
END
```

```
      SUBROUTINE BREW (LU)
      REWIND LU
      RETURN
      END
```

```
      SUBROUTINE BEND (LU)
      ENDFILE LU
      RETURN
      END
```

APPENDIX C

"Observing Systems Simulation and Potential Impact of Marine Surface Wind Data on Numerical Weather Prediction", by M. Cane, V. Cardone, M. Halem, I. Halberstam, J. Ulrich. Paper submitted to Monthly Weather Review in revised form, April, 1979.